2020

The Utilization of Sex Hormone Antibodies for Screening and Separation of Trace Biological Mixtures

Kristin N. Jones
Virginia Commonwealth University

THE UTILIZATION OF SEX HORMONE ANTIBODIES FOR SCREENING AND SEPARATION OF TRACE BIOLOGICAL MIXTURES

A thesis submitted in partial fulfillment of the requirements for the degree of Master of Science

at Virginia Commonwealth University

by

KRISTIN NOELLE JONES

Bachelor of Science, Liberty University, 2018

Director: SARAH SEASHOLS-WILLIAMS

ASSISTANT PROFESSOR, DEPARTMENT OF FORENSIC SCIENCE

Virginia Commonwealth University

Richmond, Virginia

May, 2020

Acknowledgments

The author wishes to thank several people. I would like to thank my research mentor, Dr. Susan Greenspoon, and my committee members Dr. Christopher Ehrhardt, Dr. Catherine Connon, and Cathryn Shannon. I would like to thank Dr. Ehrhardt for allowing me to join his lab and for the constant feedback both he and Dr. Greenspoon offered to guide this project along. I would like to thank my parents, Susan and Douglas, for their support over the years. I could not have made it to this point without their financial and overwhelming emotional support. I would also like to thank my friends both near and far for always loving and supporting me during my best and worst even if I was not always able to reciprocate.

Abstract

THE UTILIZATION OF SEX HORMONE ANTIBODIES FOR SCREENING AND SEPARATION OF TRACE BIOLOGICAL MIXTURES

A thesis submitted in partial fulfillment of the requirements for the degree of Master of Science at Virginia Commonwealth University

by

Kristin Noelle Jones

Bachelor of Science, Liberty University, 2018

Touch or trace evidence consists of epidermal cells deposited by contact with items such as handled objects, touched surfaces, or worn clothes. This type of evidence has surpassed most other sample types submitted to forensic labs and typically consists of low quantities of DNA and multiple contributors. In this study epithelial skin cells, i.e., "touch/trace evidence," were used as they are estimated to constitute approximately half of the casework evidence items submitted for DNA analysis. For the optimization of antibody staining, male and female skin epithelial samples from donors were incubated and hybridized with antibodies of various concentrations of Alexa 488-conjugated anti-testosterone antibody (7.00E-4 µg/µL), FITC-conjugated anti-DHT antibody (4.10E-4 µg/µL) Alexa 647-conjugated anti-estradiol antibody (2.00E-4 µg/µL), and Alexa 647-conjugated anti-testosterone (5.00E-4 µg/µL) separately at varying volumes (1.25, 2.5, 5, and 10 µL). They were also hybridized with combined Alexa 488-conjugated anti-testosterone and FITC-conjugated anti-DHT antibody (1.11E-3 µg/µL) at varying volumes (2.5 and 5 µL). Antibody binding efficiency was assessed by analyzing stained single-source male, female, and control epithelial skin cells through flow cytometry to determine if the staining to the specific target was significant when compared to the unstained control. The objective was to maximize differential binding between contributors, and to increase fluorescent signal versus noise for antibody binding. Once a staining condition was established, male and female samples were collected from different individuals and stained to determine if the staining conditions were consistent with different individuals. It was determined that not all individuals could be differentiated after staining. However, if an improved signal was observed as demonstrated by an increased median fluorescence and separation between male and female samples visualized by overlaying the histograms, then the testing moved forward to FACS analysis. The results from this study demonstrate that certain contributor cell populations derived from the epidermis may be differentiated by targeting testosterone, dihydrotestosterone, and estradiol sex hormones within cell populations as demonstrated by flow cytometry. This study resulted in a protocol for differentially labeling contributors with anti-steroid antibodies when compared to the unstained controls. This study has potential application for casework samples to simplify complex trace mixtures prior to DNA profiling.

Introduction

With the increased sensitivity of forensic analysis in recent years, another type of evidence submitted to forensic laboratories for analysis has been added. In addition to items of evidence saturated with biological fluids, evidence called “touch” evidence, consisting of trace quantities of DNA, is also being submitted (1, 2). Despite the major shift in the types of evidence laboratories are receiving, techniques to help indicate the presence of trace amounts of biological material other than blood, semen and saliva such as epithelial cells are not commercially available (1, 2). To be an effective screening technique, the procedure must require: non-destructive manipulation of the sample, little to no consumption of the sample, and a rapid processing time much like the many presumptive tests for biological fluids that are commercially available (3, 4, 5). Currently, there is limited research on effective screening methods for the indication of epithelial cells in the context of touch/trace evidence (6). However, there are techniques that utilize instrumentation that exists outside the common operational protocols of forensic science laboratories which can be utilized to analyze epithelial cells, such as fluorescence-activated cell sorting (FACS). This technique, referring to the separation of cells using flow cytometry, utilizes the fluorescent or optical characteristics of cells with or without the use of antibodies or other probes that interact with specific cell targets (7).

Developing an effective screening technique is the first step in the separation of epithelial cells, and given the predilection that a large portion of touch evidence in sexual assault cases comes from male perpetrators, a technique has to be developed in order to specifically detect male cells present at scenes of those crimes. In particular, a male cell-specific screening device that is not restricted to seminal fluid would be useful by being incorporated on the front end into cell separation techniques of complex DNA mixtures of male and female cells. In order to

identify male cells derived from touch evidence rather than sperm cells, male-specific targets found primarily in skin epithelial cells must be pursued. Theoretically, male-specific hormones may be appropriate targets. Testosterone, the primary male sex hormone responsible for producing male phenotypes, may be an effective target due to its abundance in males versus females, given that male blood serum hormone levels measure approximately 10 times that of females (8, 9, 10). As a result of the higher prevalence of testosterone in the blood serum of males, the disparity in testosterone levels found in male and female blood serum may translate to other tissues and be exploited as a target in order to screen and discriminate between male cells and female cells with the use of fluorescently labeled anti-testosterone antibodies.

Testosterone is a cholesterol-based hormone and thus is fat soluble and passively passes through the cell membrane (11). Ninety-seven percent of testosterone is bound by protein carriers in the blood. Protein bound testosterone circulates via the bloodstream for thirty to sixty minutes, after which it has either been absorbed by various tissues or degraded to inactive molecules (12, 13). Once in the cytoplasm of target tissue cells, approximately 10% testosterone is reduced to dihydrotestosterone (DHT) (14). Dihydrotestosterone (DHT) is an androgen produced as a byproduct of testosterone. Testosterone is converted to the most potent natural androgen DHT by the 5α-reductase enzyme that originates from two distinct genes, 1 5a-reductase (expressed in the liver, kidney, skin, and brain) or type 2 5α-reductase (expressed strongly in the prostate, hair follicles, and liver) (15). DHT is a potent male sex hormone that is responsible for things like forming male genitalia during pregnancy.

Both testosterone and DHT can bind to the androgen receptor complex, NR3C4 (nuclear receptor subfamily 3, group C, member 4), and the entire hormone-androgen receptor complex is then transported to the nucleus (16). Testosterone not absorbed by tissues will be degraded by the

liver, and the products of this degradation will be excreted from the body (12, 13). It is unclear if buccal cells are a target of testosterone action; however, there are saliva-based testosterone tests suggesting that measurable levels of testosterone can be found in saliva (17).

The extent to which fluorescently linked reporter molecules can be used to facilitate a front-end, contributor-specific, cell screening and separation technique has been reported in preliminary work but has not been thoroughly investigated (18). In the Miller et al. report, epithelial cell male-female mixtures were successfully enhanced for male and female DNA profiles in the post-sort fraction after staining with anti-testosterone and anti-dihydrotestosterone antibodies prior to cell separation using fluorescently activated cell sorting. A key finding in this study was that male epithelial cells were not consistently labeled at a greater signal than female cells. Systematic studies to optimize cell staining with these antibodies may produce more reproducible and diverse staining patterns that can be exploited for cell sorting and possibly screening of evidence. Additionally, staining with anti-estradiol may accentuate staining pattern differences between males and females given that the estradiol levels are significantly higher in pre-menopausal women than in men, although the levels do vary with the days of a woman's menstrual cycle (19).

In this study, skin epithelial cells are utilized, i.e., "touch/trace evidence," because skin is a target tissue of testosterone and touch/trace evidence constitutes approximately half of the casework evidence items submitted for DNA analysis (1, 20). Moreover, touch/trace evidence is typically comprised of multiple contributors, which often confounds interpretation by STR profiling (21). Thus, anti-testosterone antibody (anti-T) binding to epithelial skin cells was optimized in a systematic fashion in order to facilitate contributor specific cell staining and potential enhancement of one cell population over another. Moreover, to facilitate cell separation,

the use of counterstaining with anti-dihydrotestosterone (anti-DHT) antibodies was explored. Following the optimization of sex-hormone antibodies, DNA staining was performed in order to determine if a correlation could be made between DNA staining and hormone staining in the skin epithelial cells.

This project evaluated and systematically optimized cell staining with these antibodies. The goals were: 1) to optimize staining of each antibody separately and determine if the staining to the specific target is significant when compared to the unstained control, 2) to pair antibodies demonstrated to produce a fluorescent signal above background and determine if pairing the antibodies enhances the signal intensity (e.g. anti-testosterone and anti-DHT) or facilitates more distinct staining patterns for male epithelial cells versus female cells (e.g. anti-testosterone or anti-DHT and anti-estradiol), 3) to assess whether staining with pairs of antibodies enhances the cell sorting process, and 4) to quantify the results of cell sorting by statistical analysis, DNA profiling, and probabilistic modeling. The primary objective of this study was to optimize the experimental conditions for binding fluorescently labeled anti-testosterone, anti-DHT, and anti-estradiol antibodies to skin epithelial cells.

Research Materials and Methods

1. Sample Collection

Epithelial skin cells were collected from consenting male and female volunteers using two different methods: Whatman® FTA® Sterile Omni Swabs (GE Healthcare, Chicago, IL) and 50 mL conical tubes. Volunteers swabbed the sides of their nose and behind their ears for approximately 30 seconds with Omni Swabs in order to maximize DNA yield. Additionally, volunteers gripped conical tubes in their hands for five minutes, regularly twisting to maximize cell yield. For all samples collected, informed consent was obtained pursuant to VCU-IRB

Protocol ID#HM20000454_CR6.

2. Optimizing Antibody Staining using Anti-Testosterone

For the optimization of antibody staining, four male and four female skin epithelial samples were incubated and hybridized with Alexa 488-conjugated anti-testosterone antibody with a concentration of 7.00E-4 µg/µL (Novus Biologicals, Centennial, CO) at varying volumes (0, 2.5 µL (1.75E-3 µg), 5 µL (3.5E-3 µg), and 10 µL (7.0E-3 µg) of antibody. For the antibody staining experiments, epithelial cells were eluted into 2 mL of FACS buffer (1x PBS, 2% FBS, 0.1% sodium azide), washed once, centrifuged at 10,000xg for 10 minutes, and the supernatant was then decanted to leave 100 µL of buffer. Then 1 µL of blocking buffer (aqueous buffer, proteins, 0.09% sodium azide) (Thermo Fisher Scientific, Waltham, MA) was added to the cell suspension with gentle mixing and incubated for 10 minutes on ice. Following the incubation, varying volumes of Alexa 488-conjugated anti-testosterone antibody (Novus Biologicals) were added followed by gentle mixing. The solution was then incubated on ice for one hour with vortexing every 15 minutes. Following the incubation, the cell pellet was washed twice with 1 mL of FACS buffer, prior to flow cytometry analysis.

Antibody binding efficiency was assessed by analyzing stained single-source male and female epithelial skin cells through the use of the Guava® flow cytometer (Millipore Inc., Burlington, MA). Controls consisted of unstained male and female epithelial cells. Flow Cytometry Standard (.fcs) data files were analyzed to generate histograms using the FlowJo® software program (BD, Franklin Lakes, NJ). The median fluorescence of the male (blue) and female (pink) subpopulations stained with anti-testosterone antibody is indicated by a star in Figure 1. The percent of cells not overlapping at various fluorescence intensities in the histograms as indicated by the arrow can be used to assess if differences in fluorescence exist

between male and female fractions. The x-axis of the histogram representing fluorescence intensity was plotted against a y-axis of cell count. Using this data, statistical significance between male and female samples was determined by performing Two-Sample T-tests of Unequal Variances using Excel with an alpha of 0.01. This experiment was replicated three more times with different donors.

3. Testing and Optimizing Anti-DHT

Anti-DHT staining was optimized as described above for anti-testosterone staining; four male and four female skin epithelial samples were incubated and hybridized with FITC-conjugated anti-DHT with a concentration of 4.10E-4 µg/µL (Novus Biologicals) at varying volumes (0, 2.5 µL (1.03E-3 µg), 5 µL (2.1E-3 µg), and 10 µL(4.1E-3 µg) of antibody. Antibody binding efficiency was assessed by analyzing the average median fluorescence calculated from exported Guava® easyCyte™ data. In addition, differences in fluorescence were determined by the previously mentioned statistical analysis, with significant differences between male and female cell populations being a p-value of less than 0.01.

If an enhanced signal, demonstrated by an increased median fluorescence separation between contributor cell populations visualized by overlaying the histograms, was observed as well as a significant difference measured by statistical analysis data, then the testing moved forward to FACS analysis.

4. Counterstaining with Anti-Testosterone and Anti-DHT

Regardless if the testing and optimization of anti-DHT proved successful, the optimized probes of anti-testosterone and anti-DHT became a combined protocol for staining to determine if pairing the antibodies enhanced the signal intensity, facilitating more distinct staining patterns for male versus female epithelial cells. Using three male and three female skin epithelial

samples, enhanced antibody signal from counterstaining was assessed with the Guava® easyCyte™ flow cytometer for anti-testosterone and anti-DHT at varying volumes (0, 2.5 µL (2.78E-3 µg) and 5 µL (5.55E-3 µg) of antibody. Flow Cytometry Standard data files were analyzed as previously described. The results from the Guava® easyCyte™ flow cytometer with both antibodies were then compared to previous results generated for anti-testosterone and anti-DHT individually. Using this data, statistical significance between male and female samples was determined as previously described. This experiment was replicated one more time with different sample donors.

If when overlaying the male and female sample histograms an enhanced signal was observed demonstrated by an increased median fluorescence separation and was calculated from exported Guava® easyCyte™ data, then the testing moved forward to FACS analysis.

5. Testing and Optimizing Anti-Estradiol

Staining cells using Alexa 647-conjugated anti-estradiol antibody (Novus Biologicals, Centennial, CO) was performed because it has a different fluorescent tag and excitation range than FITC-conjugated antibodies. In addition, its prevalence in women versus men is far greater regardless of the varying levels in women during their menstrual cycle (19). Antibody probe binding efficiency conditions were optimized for anti-estradiol antibody with a concentration of 2.00E-4 µg/µL as described previously for anti-testosterone at varying volumes (0, 1.25 µL (2.5E-4 µg), 2.5 µL (5.0E-4 µg), and 5 µL (1.0E-3 µg) of antibody, using four male and four female skin epithelial cell samples. Staining was assessed using the BD FACSCanto™ II flow cytometer (BD) as anti-estradiol is conjugated with Alexa 647, which required a laser with a 633 nm output that the Guava® easyCyte™ did not possess. Cytometry Standard data files were analyzed and statistical significance between male and female samples was determined as

previously described. This experiment was replicated one more time with different sample donors.

6. Cell Permeabilization Experiment using Triton-X

In order to increase permeabilization of the epithelial cell membranes and thus theoretically increase antibody staining, a cell permeabilization experiment using Triton-X was conducted. For the permeabilization experiment, epithelial cells from six male and six female samples were eluted into 2 mL of FACS buffer, centrifuged at 10,000xg for 10 minutes, and then the supernatant was removed leaving the pellet. Two PBS Triton-X solutions were made with solution one being 4 mL PBS with 4 µL Triton-X added, and solution 2 being 4 mL with 16 µL Triton-X added. From solution one, 2 mL was pipetted into one male and one female sample. From solution two, 2 mL was pipetted into one male and one female sample. For the remaining two samples, 2 mL of PBS was added. All twelve samples were incubated at room temperature for 10 minutes. Following the incubation, the samples were centrifuged at 10,000xg for 10 minutes, and then the supernatant was removed leaving the pellet. Then 1 mL PBS was added to the samples which were again centrifuged at 10,000xg for 10 minutes. The samples were washed two more times following the same procedure. After the third wash, the supernatant was removed leaving 100 µL. Then 1 µL of blocking buffer was added to the cell suspension with gentle mixing and incubated for 10 minutes on ice. Following the incubation, 2.5 µL (1.75E-3 µg) of Alexa 488-conjugated anti-testosterone antibody (Novus Biologicals, Littleton, CO) was added to three of both the male and female samples followed by gentle mixing. The solution was then incubated on ice for one hour, and vortexed every 15 minutes. Following the incubation, the cell solution was centrifuged at 10,000xg for 10 minutes, the supernatant was removed leaving the pellet, then 500 µL of PBS was added and vortexed.

Cell permeabilization and antibody binding efficiency was assessed by analyzing stained single-source male and female epithelial skin cells through the use of the Guava® flow cytometer. Flow cytometry data files were analyzed and statistical tests were performed as previously described. This experiment was replicated one more time using different sample donors.

7. AMNIS® Imaging Flow Cytometry

Imaging flow cytometry was used to assess whether a subpopulation of cells was stained with the antibodies and how uniformly the cells were being stained. Imaging Flow Cytometry was used to answer these questions. Single-source male and female epithelial skin cells were analyzed through the use of the AMNIS® ImageStream®X Mark II (Millipore Inc., Burlington, MA) equipped with a 488 nm and 642 nm laser. Images of individual events were captured in detector channels labeled: 2 (430-505nm) and 5 (640-745nm). Channel 1 was used to capture Brightfield images, Channel 2 was the target channel for cells stained with anti-testosterone because of the 488 fluorophore, and Channel 5 was the target channel for cells stained with anti-estradiol because of the 647 fluorophore. Magnification was set at 40x and autofocus was enabled so that the focus varied with cell size. Controls consisted of unstained male and female epithelial cells.

Raw image file (.rif) data obtained from the AMNIS® instrument were analyzed using the IDEAS® v. 6.0 Image Data Exploration and Analysis software program (IDEAS®) (Millipore Inc.). For the purposes of the following AMNIS® experiments intensity, max pixel, and bright detail intensity conditions were utilized. Intensity is the sum of background subtracted pixel values within the area of the image. Max Pixel is the largest value of background-subtracted pixels contained in an image; it is more sensitive than intensity and identifies true positive

events. Bright Detail Intensity computes the intensity of localized bright spots in the area of the image as observed in Figure 2.

7.1. AMNIS® Laser Power Experiment

This experiment was performed to determine how the different laser powers affect the visualization of the antibody staining patterns. The higher the laser power the potentially more staining pattern detail observed in the cell. The ability to resolve differences in antibody staining patterns (or spatial distribution) may differ between the same antibody concentration and different laser power settings. To test which laser power results in the greatest number of in-focus large cell images in the IDEAS® software for each antibody used, four male and four female skin epithelial samples from donors were incubated and hybridized with Alexa 488-conjugated anti-testosterone antibody (0, and 2.5 µL (1.75E-3 µg) and Alexa 647-conjugated anti-estradiol antibody (0, and 2.5 µL (5.0E-4 µg). For the antibody staining experiments, epithelial cells were eluted into 2 mL of FACS buffer, centrifuged at 10,000xg for 10 minutes, and the supernatant was removed leaving 100 µL of buffer. Then 1 µL of blocking buffer was added to the cell suspension with gentle mixing followed by incubation for 10 minutes on ice (Thermo Fisher Scientific, Waltham, MA). Following the incubation, varying concentrations of antibody were added followed by gentle mixing. The solution was then incubated on ice for one hour and vigorously vortexed every 15 minutes. Following the incubation, the cell solution was washed twice with 1 mL of FACS buffer, prior to analysis.

Antibody binding efficiency was assessed by analyzing stained single-source male and female epithelial skin cells through the use of the IFC. Controls consisted of unstained male and female epithelial cells. For this experiment two laser power conditions were being assessed for each antibody. For the anti-testosterone condition one: 405nm laser was set to 50 mW, 488nm

laser to 50 mW, 561nm laser was off, and 642nm laser was off. Condition two: 405nm laser was set to 120 mW, 488nm laser to 150 mW, 561nm laser was off, and 642nm laser was off. For the anti-estradiol condition one: 405nm laser was set to off, 488nm laser was off, 561nm laser to 50 mW, and 642nm laser to 50 mW. Condition two: 405nm laser was set to off, 488nm laser was off, 561nm laser to 100 mW, and 642nm laser to 150 mW. Data obtained from the AMNIS® instrument was analyzed using the IDEAS® software program. This experiment was replicated one more time with different sample donors.

7.2. AMNIS® Antibody Visualization Experiment

This experiment was performed to determine which antibody concentration has higher values for intensity, max pixel, and bright detail intensity conditions compared to unstained cells, and gives the ability to visualize differences in antibody staining patterns with each antibody concentration with the different antibodies. Three male and three female skin epithelial samples were incubated and hybridized with Alexa 488-conjugated anti-testosterone antibody (0, 2.5 µL (1.75E-3 µg), and 5 µL (3.5E-3 µg) of antibody or Alexa 647-conjugated anti-estradiol antibody (0, 2.5 µL (5.0E-4 µg), and 5 µL (1.0E-3 µg) of antibody following the same procedure described above for the AMNIS® laser power experiment.

Antibody binding efficiency was assessed by analyzing stained single-source male and female epithelial skin cells through the use of the AMNIS® ImageStream®X Mark II. Controls consisted of unstained male and female epithelial cells. Optimal laser power for each antibody were set based on the results of the laser power experiment. Data obtained from the AMNIS® instrument was analyzed using the IDEAS® software program. This experiment was replicated one more time with different sample donors.

7.3. Using Ideas® Software to Target Nucleated Cells

For the purposes of the following AMNIS® experiment, masks and features were utilized to determine the possibility of isolating cells with potential nuclei. A mask defines a specific area of an image to use for displaying feature-value calculations. A feature is described by a mathematical expression that contains quantitative and positional information about the image and defines a set of base features that you can use to create features for each object. Data previously obtained from the AMNIS® instrument that contains potential nuclei was analyzed using the IDEAS® software program.

8. DNA Staining Assessed with the AMNIS®

GelGreen® Nucleic Acid Gel Stain (Thermo Fisher Scientific, Waltham, MA) was selected for DNA staining because it has a sensitivity lower than 0.5 ng, is also nontoxic, inexpensive, and stable at room temperature. This stain was compared to the SYBR™ Safe DNA Gel Stain (Thermo Fisher Scientific, Waltham, MA) which is highly sensitive and specifically formulated to be a less hazardous alternative to ethidium bromide that can utilize either blue light or UV excitation.

8.1. Optimizing Alexa 647-Conjugated Anti-Testosterone

GelGreen® has the same excitation range as Alexa 448-conjugated anti-testosterone in which the 488 nm laser is used. In order to simultaneously observe DNA staining with GelGreen® and antibody hybridization using anti-testosterone, an anti-testosterone antibody with a different fluorescent tag and excitation range needed to be used. Thus, antibody hybridization using Alexa 647-conjugated anti-testosterone antibody (Novus Biologicals) was performed. Antibody probe binding efficiency conditions were optimized individually first for the new anti-testosterone antibody with a concentration of 5.00E-4 µg/µL as described previously for Alexa 647-conjugated anti-estradiol by testing at varying volumes (0, 1.25 µL (6.25E-4 µg), 2.5 µL

(1.25E-3 µg), and 5 µL (2.5E-3 µg) of antibody, using four male and four female skin epithelial cell samples from sample donors. Staining was assessed using the BD FACSCanto™ II flow cytometer as this anti-testosterone was conjugated with Alexa 647, which required a laser with a 633 nm output that the Guava® easyCyte™ did not possess. Cytometry Standard (.fcs) data files were analyzed to generate histograms using the FlowJo® software program (BD, Franklin Lakes, NJ). Using this data, statistical significance between male and female samples was determined as previously described. This experiment was replicated one more time using different sample donors.

8.2. DNA Dye Optimization

For the DNA staining experiments, epithelial cells from two male and two female samples were eluted from the swabs collected from the conical tubes into 1 mL of 1 X Tris-EDTA (TE) buffer (10 mM Tris-HCl (pH 8.0), 0.1 mM EDTA), and were washed once by centrifuging at 10,000xg for two minutes to pellet the cells. The supernatant was then removed by pipetting, and the cells were resuspended in 50 µL of TE buffer. From the cell solution 3 µL was pipetted onto a glass microscope slide and dried in an incubator at 40°C for two minutes. Once the cell solution on the slide was dry, the slide was sprayed with a fixative spray to ensure the cells were fixed to the slide. Cells were then stained with 100-150 µL of GelGreen® Nucleic Acid Gel Stain or SYBR™ Safe DNA Gel Stain from a 3X dilution in sterile H_2O. The microscope slides with the dye solution were then incubated in an incubator for 30 minutes at 40°C in plastic boxes containing moistened Kimwipes® to ensure the solution on the slide did not dry out. Following the incubation, the dye solution was then washed from the slide with 2 mL of sterile H_2O.

DNA staining efficiency was assessed by analyzing stained single-source male and

female epithelial skin cells on microscope slides through the use of an Olympus BX40 comparison fluorescent microscope (Olympus Corporation, Tokyo, Japan) with a 40X objective and BV filter.

8.3. DNA Staining with GelGreen® and Antibody Hybridization

For the DNA staining experiments, epithelial cells were eluted into 2 mL of FACS buffer, washed once, centrifuged at 10,000xg for 10 minutes, and the supernatant was removed. The cells were stained with the addition of 200 µL of GelGreen® Nucleic Acid Gel Stain from a 3X dilution in sterile H_2O. The solution was incubated for 30 minutes at room temperature in the dark and vortexed every 15 minutes. Following the incubation, the cell solution with the DNA stain was washed by adding 2 mL FACS buffer and centrifuging at 10,000xg for 10 minutes. The supernatant was removed and 100 µL of FACS was added to the pellet and vortexed. Then 1 µL of blocking buffer was added to the cell suspension with gentle mixing and incubated for 10 minutes on ice. Following the incubation, varying volumes (0 and 2.5 µL (1.25 µg)) of Alexa 647-conjugated anti-testosterone antibody were added, followed by gentle mixing. The solution was then incubated on ice for one hour and vortexed every 15 minutes. Following the incubation, the cells were washed by adding 1 mL FACS buffer and centrifuging at 10,000xg for 10 minutes. The supernatant was removed and 100 µL of FACS was added to the pellet and vortexed.

DNA staining efficiency was assessed by analyzing stained single-source male and female epithelial skin cells through the use of the AMNIS® ImageStream®X Mark II. Controls consisted of unstained male and female epithelial cells. Data obtained from the AMNIS® instrument was analyzed using the IDEAS® v. 6.0 Image Data Exploration and Analysis software program.

9. Fluorescence Activated Cell Sorting (FACS)

Male-female 1:1 volume:volume epithelial cell mixtures were stained with both anti-testosterone and anti-estradiol probes and passed through the Aria-BD FACSAria™ II Cell Sorter (Beckton Dickinson, Franklin Lakes, NJ) using a 488 nm excitation laser. Data obtained from the FACS instrument were analyzed using the FACSDiva v. 6.1.3 software program (Becton Dickinson) to see how the FACS sorting performs with the antibody staining for both anti-testosterone and anti-DHT. The effectiveness of the FACS sorting was evaluated by STR profiling and probabilistic modeling to quantify the DNA testing results. This experiment was replicated one more time with different sample donors. Then DNA analysis of Pre- and Post-sorted FACS fractions was performed.

9.1. DNA analysis of Pre- and Post-sorted FACS fractions

All sorted cell fractions, as well as unsorted mixture samples (used as an initial reference), were extracted manually with the DNA IQ™ System (Promega, Madison, WI) following the protocols described in the Virginia Department of Forensic Science (VDFS) Procedures Manual (22). Purified DNA extracts (~35 µL) and reference DNA samples were dried down using vacuum centrifugation (SpeedVac, Thermo Fisher Scientific) in low-bind tubes (Thermo Fisher Scientific, Waltham, MA) and then resuspended in ~13µL with Type I water. With a few exceptions, only the reference DNA samples were quantified with Promega's PowerQuant® System (Promega Corp., Madison, WI) using Applied Biosystem's 7500 Quantitative PCR instrument (Applied Biosystems [ABI], Carlsbad, CA) following the manufacturer's recommendations. After data were collected, the PowerQuant® data were analyzed using the PowerQuant® Analysis macro provided by Promega Corp.

Short tandem repeat (STR) amplification was performed on the GeneAmp 9700 thermal cycler (ABI), using Promega's PowerPlex® Fusion System as described by the manufacturers.

Ten microliters of DNA extract were added to 15 µL of the STR reaction mix for a full volume, 25 µL reaction. STR products were separated on a 3500xl Genetic Analyzer (ABI) with a 24-second injection at 1.2 kVolts during injection (15 kVolts during run), followed by STR analysis with the GeneMapper® ID-X v1.4 or 1.5 software program (ABI) as described in the VDFS Procedures Manual (22). The analytical threshold that was used to interpret the STR profiles manually was 75 RFU for each dye channel (22).

Probabilistic genotype modeling analysis was conducted using the TrueAllele® (TA) Casework system (Cybergenetics, Pittsburgh, PA). The procedure was performed as described in the TrueAllele Casework user manuals and as described in the Virginia Department of Forensic Science procedures manual (22). The TA® Casework System can be used to aid the casework examiner in mixture analysis and likelihood ratio calculations of two, three and four person DNA mixtures. TA® Casework is a probabilistic modeling approach validated for its effectiveness with complex mixtures while preserving profile information which may be ignored with traditional binary statistical approaches.

Results

1. Optimizing Antibody Staining using Anti-Testosterone

Initial screening of epidermal cells for Alexa 488-conjugated anti-testosterone antibody probe binding was conducted on 10 different contributor cell populations (five male and five female samples). Fluorescence histograms of cell populations are shown in Figures 3 and 4. Probe binding was observed for all antibody concentrations tested as evidenced by shifts in median fluorescence between unstained and stained cell populations. The female cell populations had median fluorescence values with standard deviations of 265 ±121, 576 ±124, 556 ±128, and 659 ±116 respectively, while male cell populations had median fluorescence values of 220 ±117,

603 ±108, 656 ±95, and 660 ±104 respectively. The distribution of fluorescence values for each cell population showed significant variation between individuals with no clear systematic differences between male and female individuals, as female cell populations stained higher in some cases while male cell populations stained higher in others (Figure 4). However, some distinct subpopulations of cells with higher median fluorescence and minimal overlap in fluorescence histograms were observed as seen highlighted with an arrow in Figure 4.

A statistical comparison between male and female cell subpopulation median fluorescence values is shown in Figure 5. Following statistical testing, p-values were 7.12E-34 for 0 µL with a median difference of 45 (17%), 1.37E-14 for 2.5 µL (1.75E-3 µg) with a median difference of 27 (4.5%), 2.98E-117 for 5 µL (3.5E-3 µg) with a median difference of 100 (15%), and 0.43 for 10 µL (7.0E-3 µg) with a median difference of one (0.15%), respectively. The no antibody control provides a measure of autofluorescence signal at the measured wavelength. Overall, staining with Alexa 488 anti-testosterone antibody resulted in an increase in median fluorescence from unstained to stained cells and showed a greater median fluorescence separation between male and female cell populations with the addition of 5 µL (3.5E-3 µg) of antibody.

2. Testing and Optimizing Anti-DHT

Initial screening of epidermal cells for FITC-conjugated anti-DHT antibody probe binding was conducted on four contributor cell populations (two male and two female samples). Fluorescence histograms of cell populations are shown in Figures 6 and 7. Probe binding was observed across all antibody concentrations tested as evidenced by shifts in median fluorescence between unstained and stained cell populations (see Figures 6 and 7). The female cell populations had median fluorescence values with standard deviations of 265 ±121, 323 ±127,

336 ±113, and 372 ±115 respectively, while male cell populations had median fluorescence values of 220 ±117, 333 ±114, 361 ±120, and 390 ±110, respectively. The subpopulations of cells had neither distinct higher median fluorescence nor sufficient separation in fluorescence (Figure 7).

A statistical comparison between male and female cell subpopulation median fluorescence is shown in Figure 8. Following statistical testing, p-values were 7.12E-34 for 0 µL with a median difference of 45 (17%), 0.13 for 2.5 µL (1.03E-3 µg) with a median difference of 10 (3%), 4.32E-21 for 5 µL (2.1E-3 µg) with a median difference of 25 (7%), and 0.11 for 10 µL (4.1E-3 µg) with a median difference of 18 (4.6%) respectively. Overall, staining with FITC anti-DHT antibody resulted in only a slight increase in median fluorescence from unstained to stained cells and showed a greater median fluorescence separation between male and female cell populations with the addition of 5 µL (2.1E-3 µg) of antibody.

3. Counterstaining with Anti-Testosterone and Anti-DHT

Following the individual optimization of Alexa 488-Conjugated anti-testosterone and FITC-conjugated anti-DHT antibodies, a screening of epidermal cells for increased probe binding of the two combined antibodies was conducted on two male and two female samples. Fluorescence histograms of cell populations generated are shown in Figures 9 and 10. The female cell populations had median fluorescence values with standard deviations of 272 ±117, 574 ±106, and 614 ±108 respectively, while male cell populations had median fluorescence values of 265 ±113, 576 ±109, and 644 ±92 respectively. Probe binding was observed across all samples as evidenced by shifts in median fluorescence between unstained and stained cell populations. The distribution of fluorescence values for each cell population showed little variation between individuals with no clear systematic differences between male and female

individuals. However, some potential subpopulations of cells with higher median fluorescence and minimal overlap in fluorescence histograms were observed, as seen highlighted with arrows in Figures 10. It cannot be definitely determined visually if there is significant separation due to the lack of cells present in the male cell subpopulation at that antibody concentration.

A statistical comparison between male and female cell population median fluorescence values is shown in Figure 11. Following statistical testing, p-values were 0.96 for 0 µL with a median difference of seven (2.6%), 0.84 for 2.5 µL (2.78E-3 µg) with a median difference of two (0.35%), and 1.07E-11 for 5 µL (5.55E-3 µg) with a median difference of 30 (4.7%) respectively. Overall, when anti-testosterone and anti-DHT antibodies were paired, the median fluorescence increased between unstained and stained cell populations and showed a greater increased median fluorescence separation between male and female cell populations with the addition of 5 µL (5.55E-3 µg) of antibody.

Compared to the anti-testosterone individual optimization results, the counterstaining with anti-DHT did not increase median fluorescence intensity. Following statistical testing, p-values for the female cell populations were 0.29 for 0 µL, 0.13 for 2.5 µL (2.78E-3 µg), and 1.85E-62 for 5 µL (5.55E-3 µg) of antibody respectively. P-values for the male cell populations were 1.46E-27 for 0 µL, 2.8E-4 for 2.5 µL (2.78E-3 µg), and 1.99E-5 for 5 µL (5.55E-3 µg) of antibody respectively. However, compared to the anti-DHT individual optimization results, the counterstaining with anti-testosterone did increase the median fluorescence values of the male and female cell populations.

4. Testing and Optimizing Anti-Estradiol

Initial screening of epidermal cells for Alexa 647-conjugated anti-estradiol antibody probe binding was conducted on two male and two female samples. Fluorescence histograms of

cell populations generated in FlowJo® are shown in Figures 12 and 13. The female cell populations had median fluorescence values with standard deviations of 350 ±13, 382 ±81, 410 ±121, and 453 ±158 respectively, while male cell populations had median fluorescence values of 350 ±23, 388 ±74, 465 ±138, and 452 ±111 respectively. Probe binding was observed across all concentrations tested as evidenced by shifts in median fluorescence between unstained and stained cell populations. The distribution of fluorescence values for each cell population showed significant variation between individuals with no clear systematic differences between male and female individuals as female cell populations stained higher in some cases while male cell populations stained higher in others. However, some distinct subpopulations of cells with higher median fluorescence and minimal overlap in fluorescence histograms were observed as seen highlighted with arrows in Figure 13. Previous work has observed that the fluorescent signal of unstained epithelial cells was greater when utilizing the 633 nm wavelength for fluorophore detection due to epithelial cell autofluorescence (23).

A statistical comparison between male and female cell population median fluorescence values is shown in Figure 14. Following statistical testing, p-values were 0.19 for 0 µL with a median difference of zero (0%), 0.63 for 1.25 µL (2.5E-4 µg) with a median difference of six (1.5%), 1.37E-11 for 2.5 µL (5.0E-4 µg) with a median difference of 55 (11.8%), and 2.29E-6 for 5 µL (1.0E-3 µg) with a median difference of one (0.22%) respectively. Overall, the results for anti-estradiol antibody staining showed a greater increased median fluorescence separation between male and female cell populations with the addition of 2.5 µL (5.0E-4 µg) of antibody.

5. Cell Permeabilization Experiment using Triton-X

Cell permeabilization of epidermal cells with Triton-X using Alexa 488-conjugated anti-testosterone antibody was conducted on two male and two female samples. Fluorescence

histograms of cell populations are shown in Figure 15. Probe binding was observed across all samples as evidenced by shifts in median fluorescence between unstained and stained cell populations in the histograms. The subpopulations of cells had neither distinct higher median fluorescence nor sufficient separation in fluorescence.

A statistical comparison between male and female cell subpopulation median fluorescence is shown in Figure 16. Following statistical testing, p-values were 7.66E-4 with a median difference of 327 (27%), 3.30E-31 with a median difference of 260 (28%), 6.93E-40 with a median difference of 207 (24.8%), 1.42E-13 with a median difference of 3,111 (13%), 0.02 with a median difference of 758 (3.3%), and 0.16 with a median difference of 1,431 (5.5%) respectively. Overall, male and female cells stained with 2.5 µL (1.75E-3 µg) of antibody have a higher median fluorescence compared to unstained cells. However, there is no difference in the median fluorescence of male and female cells with the addition of Triton-X. Thus, Triton-X either did not increase permeability of the epithelial cells, or cell permeabilization had no effect on antibody staining.

6. AMNIS® Imaging Flow Cytometry

6.1. AMNIS® Laser Power Experiment

In order to also analyze antibody hybridization for epidermal cell samples using imaging flow cytometry, laser power (illumination intensities) needed to be tested in order to determine which condition resulted in the greatest number of in-focus large cell images in the Ideas® Software for each antibody used.

6.1.1. Anti-Testosterone

In regards to the cell images, there are both the brightfield and fluorescence imaging of two individual female and male epidermal cells that have been hybridized with Alexa 488-

conjugated anti-testosterone probes, with the 488 nm laser at 50 mW (condition 1) and 150 mW (condition 2), and channel 2 (430-505nm) being the channel of interest because of the 488 fluorophore tagged to the antibody (Figure 17). Table 1 compares male and female cell subpopulation mean intensity, max pixel, and bright detail intensity values of anti-testosterone AMNIS® laser power experiment experiments. The stained male cells at 50 mW had intensity of 2.33E5, max pixel of 1.55E2, and bright detail intensity of 8.53E3 while at 150 mW the cells had intensity of 4.74E5, max pixel of 2.99E2, and bright detail intensity of 1.32E4. The stained female cells at 50 mW had intensity of 1.71E5, max pixel of 3.17E2, and bright detail intensity of 1.43E4 while at 150 mW the cells had intensity of 3.75E5, max pixel of 7.73E2, and bright detail intensity of 4.76E4.

For both laser power conditions tested, both male and female cells stained with 2.5 µL (1.75E-3 µg) of Alexa 488 anti-testosterone had higher values for intensity, max pixel, and bright detail intensity conditions compared to unstained cells. Both male and female cells captured with 150 mW illumination power have higher values for intensity, max pixel, and bright detail intensity conditions compared to cells captured with 50 mW illumination power as expected with increased laser power. Since an increased laser power should also result in increased intensity values, the primary focus in the scope of this experiment should be bright detail intensity. Bright detail intensity is more than a measurement of intensity, it also reflects spatial heterogeneity of pixels across the cell. Based on the bright detail intensity value which increased from 8.53E3 to 1.32E4 in males and from 1.43E4 to 4.76E4 in female, condition two (405nm laser set at 120 mW, 488nm laser at 150 mW, 561nm laser was off, and 642nm laser was off) will be used with anti-testosterone stained cells.

6.1.2. Anti-Estradiol

In regards to the cell images, there are both the brightfield and fluorescence imaging of two individual female and male epidermal cells that have been hybridized with Alexa 647-conjugated anti-estradiol probes, with the 642 nm laser set to 50 mW (condition 1) and 150 mW (condition 2), and channel 5 (640-745nm) being the channel of interest (Figure 18). Table 2 numerically compares male and female cell subpopulation mean intensity, max pixel, and bright detail intensity values of anti-estradiol for the AMNIS® laser power experiment runs. The stained male cells at 50 mW had intensity of 1.29E5, max pixel of 8.06E1, and bright detail intensity of 1.52E4 while at 150 mW the cells had intensity of 2.26E5, max pixel of 2.10E2, and bright detail intensity of 2.96E4. The stained female cells at 50 mW had intensity of 1.97E5, max pixel of 1.40E2, and bright detail intensity of 2.19E4 while at 150 mW the cells had intensity of 5.03E5, max pixel of 4.11E2, and bright detail intensity of 4.86E4.

For both laser power conditions, male and female cells stained with 2.5 µL (5.0E-4 µg) of Alexa 647 anti-estradiol had higher values for intensity, max pixel, and bright detail intensity conditions compared to unstained cells. Both male and female cells captured with 150 mW illumination power have higher mean values for intensity, max pixel, and bright detail intensity conditions compared to cells captured with 50 mW illumination power as expected with increased laser power. As previously stated, bright detail intensity was the primary focus. Based on the bright detail intensity value which increased from 1.52E4 to 2.96E4 in males and from 2.19E4 to 4.86E4 in female, condition two (405nm laser set at 120 mW, 488nm laser at 150 mW, 561nm laser was off, and 642nm laser was off) will be used with anti-testosterone stained cells. Female cells have higher mean values than male cells for intensity, max pixel, and bright detail intensity conditions. Condition two (405nm laser was off, 488nm laser was off, 561nm laser set to100 mW, and 642nm laser set to 150 mW) will be used with anti-estradiol stained cells.

6.2. AMNIS® Antibody Visualization Experiment

6.2.1. Anti-Testosterone

After determining what laser power is most effective with the 488 nm laser for Alexa 488-conjugated anti-testosterone, the next step was to determine which antibody concentration has higher values for intensity, max pixel, and bright detail intensity conditions compared to unstained cells and shows the greatest discrepancy between male and female cells. In regards to the cell images, there are both the brightfield and fluorescence imaging of individual female and male epidermal cells that have been hybridized with Alexa 488-conjugated anti-testosterone probes, with the unstained (top), stained with 2.5 µL (1.75E-3 µg) antibody (middle), and stained with 5 µL (3.5E-3 µg) antibody (bottom) (Figure 19). Something of particular interest was noted in the male sample seen in Figure 19, for the cell stained with 2.5 µL (1.75E-3 µg) antibody (middle) appeared to potentially have a nucleus which fluoresced brighter than the rest of the cell. This same feature was observed in other cells in this particular sample. Also something to note, the cell does fluoresce in all channels indicating some autofluorescence at the various wavelengths.

Overall, both male and female cells stained with Alexa 488 anti-testosterone have higher values for intensity, max pixel, and bright detail intensity conditions compared to unstained cells. As previously stated, bright detail intensity is the primary focus. Based on the bright detail intensity value which at 2.5 µL (1.75E-3 µg) was 2.28E4 for males and 2.99E4 for females with a difference of 7,100, and at 5 µL (3.5E-3 µg) was for 2.61E4 males and 6.91E4 for females with a difference of 43,000. Cells stained with 5 µL (1.75E-3 µg) of anti-testosterone have higher values for all three conditions compared to 2.5 µL (1.75E-3 µg), and there is greater discrepancy between male and female cells with 5 µL (1.75E-3 µg) of antibody added based on the difference

in bright detail intensity values.

6.2.2. Anti-Estradiol

After determining what laser power is most effective with the 643 nm laser for Alexa 647-conjugated anti-estradiol, the next step was to determine which antibody concentration has higher values for intensity, max pixel, and bright detail intensity conditions compared to unstained cells and displays the greatest discrepancy between male and female cells. As previously stated, bright detail intensity is the primary focus. In regards to the cell images, there are both the brightfield and fluorescence imaging of individual female and male epidermal cells that have been hybridized with Alexa 647-conjugated anti-estradiol probes, with the unstained (top), stained with 2.5 µL (5.0E-4 µg) antibody (middle), and stained with 5 µL (1.0E-3 µg) antibody (bottom) (Figure 20). For both the male and female samples, fluorescence is observed with cells that have a size and morphology consistent with epidermal cells.

Overall, both male and female cells stained with Alexa 647 anti-estradiol have higher values for intensity, max pixel, and bright detail intensity conditions compared to unstained cells. Based on the bright detail intensity value which at 2.5 µL (5.0E-4 µg) was 4.4E4 for males and 3.74E4 for females with a difference of 6,600, and at 5 µL (1.0E-3 µg) was for 5.49E4 males and 5.77E4 for females with a difference of 2,100. While cells stained with 5 µL (1.0E-3 µg) of anti-estradiol have higher values for all three conditions compared to 2.5 µL (5.0E-4 µg), there is greater discrepancy between male and female cells with 2.5 µL (5.0E-4 µg) of antibody added based on the difference in bright detail intensity values.

6.2.2.1. Anti-Testosterone vs. Anti-Estradiol

Following the initial screening and optimization of epidermal cells using the Alexa 488-conjugated anti-testosterone and Alexa 647-conjugated anti-estradiol antibodies, male and

female cell populations were compared with respect to intensity, max pixel, and bright detail intensity using optimized antibody conditions (Figure 21). As previously stated, bright detail intensity is the primary focus. Female cells stained with both 2.5 and 5 µL of both anti-testosterone and anti-estradiol have higher values for intensity, max pixel, and bright detail intensity conditions compared to unstained cells. The anti-testosterone stained female cells at 2.5 µL (1.75E-3 µg) had intensity of 6.99E5, max pixel of 4.94E2, and bright detail intensity of 2.99E4 while at 5 µL (3.5E-3 µg) the cells had intensity of 6.98E5, max pixel of 8.36E2, and bright detail intensity of 6.91E4. The anti-estradiol stained female cells at 2.5 µL (5.0E-4 µg) had intensity of 3.24E5, max pixel of 4.38E2, and bright detail intensity of 3.74E4 while at 5 µL (1.0E-3 µg) the cells had intensity of 5.85E5, max pixel of 7.04E2, and bright detail intensity of 5.77E4. For intensity, max pixel, and bright detail intensity conditions p-values for 2.5 µL of antibody were 2.05E-6 for intensity, 0.13 for max pixel, and 0.02 for bright detail intensity, while p-values for 5 µL of antibody were 0.66 for intensity, 0.66 for max pixel, and 0.76 for bright detail intensity. Based on the bright detail intensity p-value of 0.02 at 2.5 µL of antibody, anti-testosterone stained female cells have higher values than anti-estradiol stained cells.

Male cells stained with both 2.5 and 5 µL of both anti-testosterone and anti-estradiol have higher values for intensity, max pixel, and bright detail intensity conditions compared to unstained cells. The anti-testosterone stained male cells at 2.5 µL had intensity of 3.65E5, max pixel of 3.37E2, and bright detail intensity of 2.28E4 while at 5 µL the cells had intensity of 3.98E5, max pixel of 4.07E2, and bright detail intensity of 2.61E4. The anti-estradiol stained male cells at 2.5 µL had intensity of 3.78E5, max pixel of 5.46E2, and bright detail intensity of 4.40E4 while at 5 µL the cells had intensity of 5.53E5, max pixel of 7.33E5, and bright detail intensity of 5.49E4. Anti-estradiol stained cells have higher values than anti-testosterone stained

cells for intensity, max pixel, and bright detail intensity conditions. For intensity, max pixel, and bright detail intensity conditions, p-values for 2.5 µL of antibody were 0.73 for intensity, 5.78E-5 for max pixel, and 5.01E-6 for bright detail intensity, while p-values for 5 µL of antibody were 0.01 for intensity, 0.001 for max pixel, and 2.93E-5 for bright detail intensity. Based on the bright detail intensity p-value of 5.01E-6 at 2.5 µL and 2.93E-5 of antibody at 5 µL, anti-estradiol stained male cells have higher values than anti-testosterone stained cells.

Table 3 compares the antibody visualization results on AMNIS® to the antibody optimization results on the flow cytometers. For the cells stained with anti-testosterone, the antibody concentration with the greatest discrepancy between male and female cell populations on Guava® was 5 µL and on the AMNIS® it was 5 µL. This demonstrates that the anti-testosterone Guava® and AMNIS® results were consistent, meaning that the data generated from the flow cytometer was consistent with the data visualized with the imaging flow cytometer.

Comparing the antibody visualization results on AMNIS® to the antibody optimization results on the flow cytometers for the cells stained with anti-estradiol, the antibody concentration with the greatest discrepancy between male and female cell populations on Guava® was 2.5 µL and on the AMNIS® it was 2.5 µL as well. This data demonstrates that the anti-estradiol Guava® and AMNIS® results were consistent.

6.3. Using Ideas® Software to Target Nucleated Cells

Following the AMNIS® visualization experiments, where some nuclei were observed in cell images, an attempt was made to isolate cells with nuclei utilizing morphological and/or optical features. Being able to isolate cells with nuclei can help one better understand visually how antibodies interact in the cell where that antibody is synthesized, and demonstrates that some skin epithelial cells contain intact nuclei where DNA would be present. During this

experiment cell images 60 and 127, which contained nuclei, were used as the templates for developing features to target potential nuclei in other samples.

Figure 22, a screenshot from the Ideas® Software, depicts cells gated using the Spot(M02, Ch02, Bright, 5.88, 9, 4) mask. The spot mask is the bright option that obtains bright regions from an image regardless of the intensity differences from one spot to another. Using this mask, both cell images 60 and 127 were included in the nuclei gate. However, in total there were 233 cell events also included in that gate that did not contain nuclei, making this mask too general.

Figure 23, a screenshot depicting cells gated using the Intensity(M02, Ch02, 250-500) mask. The intensity mask uses pixels between the lower and upper raw intensity thresholds in a specified range to generate data. Using this mask, only cell image 127 was included in the nuclei gate. While the number of cells included in the nuclei gate was reduced to 18 cell events, the gate did not include cell image 60 so this mask was not suitable to use as it may exclude some cells with nuclei.

Figure 24, a screenshot from the Ideas® Software, depicts cells gated using the combined Spot(M02, Ch02, Bright, 5.88, 9, 4) And Intensity(M02, Ch02, 250-500) mask. This mask combines the two previously described masks. Using this mask, both cell images 60 and 127 were included in the nuclei gate. However, there were a total of 370 cell events also included in that gate that did not contain nuclei, making this mask too general.

Figure 25, a screenshot from the Ideas® Software, depicts cells gated using the combined Spot (M02, Ch02, Bright, 5.88, 9, 4) And Morphology(M02, Ch02) mask. This mask combines a previously described mask as well as morphology, which is used in fluorescence images and best used for calculating the values of overall shape-based features. Using this mask, both cell images 60 and 127 were included in the nuclei gate. However, there were a total of 370 cell events also

included in that gate that did not contain nuclei, making this mask too general.

Figure 26 depicts cells gated using the combined Component 1, (Circularity, Spot(M02, Ch02, Bright, 5.88, 9, 4), Ascending) mask. This mask combines a previously described mask as well as circularity, which measures the degree of the mask's deviation from a circle. The closer the object to a circle the smaller the variation, and therefore, the feature value will be high. Using this mask, only cell image 127 was included in the nuclei gate. While the number of cells included in the nuclei gate was reduced to 77 cell events, because the gate did not include cell image 60, this mask was not suitable to use as it may exclude some cells with nuclei.

Table 4 summarizes all of the Ideas® Software data from each gate used to target nucleated cells. For the Spot(M02, Ch02, Bright, 5.88, 9, 4) mask in total there were 233 cell events included in that gate that did not contain nuclei in addition to the two cell that did, however, it contained both target cells as well as the least number of other non-target cells, making it best suited to isolate cells with potential nuclei.

7. DNA Staining Assessed with the AMNIS®

Due to unforeseen issues that occurred with FACS sorting, it was not possible to assess whether staining with pairs of antibodies enhances the cell sorting process and thus results of cell sorting could not be quantified by statistical analysis or probabilistic modeling. Following the issues with FACS sorting, it was decided to try DNA staining on AMNIS® using a new antibody, Alexa 647-conjugated anti-testosterone, which had the greatest separation between male and female cell populations of all the antibodies used.

7.1. Optimizing Alexa 647-Conjugated Anti-Testosterone

Initial screening of epidermal cells for Alexa 647-conjugated anti-testosterone antibody probe binding was conducted on two male and two female samples. Fluorescence histograms of

cell populations generated in FlowJo® are shown in Figures 27 and 28. Probe binding was observed across all concentrations tested as evidenced by shifts in median fluorescence between unstained and stained cell populations. The female cell populations had median fluorescence values with standard deviations of 2463 ±3887, 15695 ±18682, 26728 ±34146, and 51801 ±59324, respectively, while male cell populations had median fluorescence values of 2084 ±2130, 6140 ±10474, 8940 ±11937, and 15445 ±18506, respectively. Interestingly, the fluorescent signal of unstained epithelial cells was greater when utilizing the 633 nm wavelength compared to the 488 nm wavelength for fluorophore detection, likely due to epithelial cell autofluorescence (22). However, some distinct subpopulations of cells with higher median fluorescence and minimal overlap in fluorescence histograms were observed as seen in Figure 28.

A statistical comparison between male and female cell subpopulation median fluorescence calculated from exported Canto data is shown in Figure 29. Following statistical testing, p-values were 1.79E-44 for 0 µL with a median difference of 379 (16%), 0.00 for 1.25 µL (6.25E-4 µg) with a median difference of 9,555 (60.9%), 0.00 for 2.5 µL (1.25E-3 µg) with a median difference of 17,788 (66.6%), and 0.00 for 5 µL (2.5E-3 µg) with a median difference of 36,356 (70.2%) respectively. Overall, the results for anti-testosterone antibody staining showed a greater increased median fluorescence separation between male and female cell populations with the addition of 2.5 µL (1.25E-3 µg) of antibody.

Overall, female and male cells stained with Alexa 647 anti-testosterone have higher median fluorescence than all other antibody-stained cells at all antibody concentrations, and the greatest discrepancy between male and female cells making it the best antibody for hybridization.

7.2. DNA Dye Optimization

Once the Alexa 647 anti-testosterone antibody was optimized, a comparison was then conducted between the GelGreen® Nucleic Acid Gel Stain and SYBR™ Safe DNA Gel Stain, both of which are sensitive commercially available DNA stains. Once the optimal excitation filter on the microscope was determined, two male and two female donors were stained with GelGreen® and SYBR™ Safe to determine which would best stain skin epithelial cells to be observed with AMNIS®. Upon comparison it was determined that both DNA stains fluoresced equally, and so GelGreen® was chosen for the DNA staining experiment on AMNIS® because of its safer non-mutagenic properties.

7.3. DNA Staining with GelGreen® and Antibody Hybridization

Following the optimization of the DNA stains and determination to move forward with the GelGreen® stain for the experiment on AMNIS®, male and female cell samples were prepared using the combined DNA stain and antibody hybridization protocol. The male and female samples were run on the AMNIS®, however, because this sort of experiment has yet to be published in literature it was unsure how the results would turn out. It was expected that the GelGreen® would fluoresce in the green channel while the Alexa 647 anti-testosterone antibody would fluoresce in the red channel. However, this was not the case as the antibody did not fluoresce at all. It was determined that more would need to be done with the DNA staining experiment in order to determine the best way to effectively combine the two protocols.

8. Fluorescence Activated Cell Sorting (FACS)

Following antibody staining optimization using flow cytometers and antibody visualization utilizing the AMNIS®, it was decided to move forward with FACS sorting using anti-testosterone and anti-estradiol. Figure 30 displays the FACS sorting data with anti-

testosterone (left) and anti-estradiol (right). Both the reports for the anti-testosterone antibody and the anti-estradiol show an apparent single peak in the histograms of the 1:1 male:female mixtures rather than two separate peak populations. These results contradict earlier results found in the Miller et al. report where two distinct peaks were observed in the FACS gate histograms.

When the sorted male and female cell fractions were subjected to DNA analysis and the results were analyzed, no male DNA was present in the electropherograms. This could be the result of improper mixing when aliquoting pre- and post-sort fractions or biological factors of the male epidermis stratum corneum skin layer. As a result of two failed FACS sorts, a new approach to the project was taken. It was determined that a DNA staining experiment be conducted in order to determine if the antibody was in the epithelial cells and if those epithelial cells contained DNA as well. This would help determine if the cells that were staining with the antibody actually contained DNA. If not, then that would help explain the lack of DNA found in post-sort samples.

When conducting the DNA staining experiment, a new antibody had to be optimized in order to simultaneously visualize antibody and DNA staining in separate AMNIS® channels. An anti-testosterone antibody with a different fluorescent tag and excitation range needed to be used as GelGreen® shared the same fluorophore as the Alexa 488-conjugated anti-testosterone. It was decided to also test this antibody, Alexa 647-conjugated anti-testosterone, with FACS sorting. Figure 31 shows the report from FACS sorting with Alexa 647-conjugated anti-testosterone that shows separation of peaks from a 1:1 male:female mixture in solution. The skin epidermal cells in the mixture were incubated with the Alexa 647 anti-testosterone antibody and physically sorted into two fractions: P5 “left” or P6 “right”. When sorted, the gated P5 fraction contained 33,204 cells and the gated P6 fraction contained 34,643 cells. Based on the Alexa 647 anti-

testosterone optimization histogram peak characteristics for both the male and female cell populations, it was expected that the P5 post-sort fraction contained the female profile, while the male profile was expected to be enriched from the P6 post-sort fraction. However, something to note is that at the 633 nm wavelength, a higher autofluorescence was observed with unstained cells which could result in P5 being autofluorescence and P6 being the stained male and female cell populations.

8.1. DNA analysis of Pre- and Post-sorted FACS fraction

After DNA typing the pre-sort mixture, P5 and P6 post-sort fractions, and male and female donor reference samples, it was determined that each sorted fraction contained alleles consistent with both male and female contributors as well as an unknown third contributor. In the pre-sort mixture STR typing profile chart depicted in Figure 32, the alleles were consistent with both the male and female contributors with a greater number of alleles attributed to the male. In the post-sort P5 fraction STR typing profile chart depicted on the left in Figure 32, the few alleles present were consistent with both the male and female contributors with a greater number of alleles attributed to the male. In the post-sort P6 fraction STR typing profile chart depicted on the right in Figure 32, the alleles were consistent with both the male and female contributors with a greater number of alleles attributed to the male. It should be noted that in the pre-sort and both post-sort fractions there were alleles not attributable to either the female or male contributors, marked with an asterisk in Figure 32. The presence of extra alleles is not unusual in trace evidence samples given the low template DNA quantity; however, some of the same non-contributor alleles can be observed in both pre-sort and post-sort fractions, suggesting that it is possible the extraneous DNA was introduced during sampling.

Following STR analysis of the samples, a quantitative assessment was performed on the

profiles to determine the uncertainty of those genotypes when comparisons were performed between reference samples and both the pre- and post-sort fractions. This quantitative assessment was done using TrueAllele® Casework (TA) analysis.

Analysis of the pre-sort mixture indicated statistical support for the male contributor in the unsorted mixture (Log(LR) 29), but no statistical support for the female contributor (Log(LR) 1.3), consistent with the large number of male alleles and the minimal number of unique female alleles observed. Interestingly, analysis for the male and female contributors in the P5 left fraction was inconclusive (both Log(LR) <0) (Table 5), consistent with the minimal number of alleles observed and excessive allelic and locus dropout. However, analysis of the P6 right fraction indicated statistical support for the male contributor (Log(LR) 9), but no statistical support for the female contributor (Log(LR) inconclusive). The P6 results were consistent with 'the large number of male alleles and the minimal number of female alleles above detection threshold.

Discussion

Overall, the results from this study show that contributor cell populations from trace biological samples may be differentiated by targeting testosterone, dihydrotestosterone, and estradiol sex hormones within forensically relevant epithelial cell samples. One unexpected result from these experiments was that epithelial cell populations from female contributors often showed higher affinity for testosterone antibody probes compared to epithelial cell populations from male contributors. Another unexpected result from these experiments was that epithelial cell populations from male contributors often showed higher affinity for estradiol antibody probes compared to epithelial cell populations from female contributors. There are several possible explanations for these unexpected results, but they complicate the cell separation and

prevent the use of a “one size fits all” application of the gating criteria.

One explanation is that hormone levels can vary between individuals of not only the different sexes but within the same sex as well due to lifestyle variables (smoking increases testosterone), changes in reproductive organ function (affected by medications), body composition, age, and ethnicity (19, 24, 25, 26, 27). For the samples collected, no information was known about the donors aside from sex pursuant to our collection protocols. As a result, it is difficult to determine if any of these explanations are the cause for the unexpected results. Another explanation is that hormone molecules within the skin’s epidermal tissue can be influenced by factors such as cellular turnover rate and biochemical profile of the epidermis (28). Yet another potential explanation is that epidermal thickness is a major factor in the ability of hormone antibodies to bind to hormones within the cell. In one study of nearly 100 individuals, it was found that males had a thicker cellular epidermis than females (29). This supports the theory that males have thicker epidermal skin layers than females, and that if the male cells are fully keratinized they are less likely to contain DNA (30).

One explanation as to why the FACS separation did not work with the DNA yield being so low in sorted cell populations is the potential prevalence of extracellular DNA (eDNA) versus intracellular DNA (31, 32, 33). Early research suggests 70% of contact samples contained eDNA which added value to the STR profiles generated from the pelleted cellular material, while later research suggests the DNA in touch samples are comprised of as much as 84-100% eDNA (31, 32). This in part impacted the resolution of the FACS separation, where the cells depicted in the histograms did not necessarily have enough DNA for effective DNA profiling. The skin epithelial cells used in this study go through a process known as keratinization, where the cells display gradual shrinking of the nucleus as they migrate towards the surface and the cells are

filled with keratin (30). As such, these cells have minimal DNA content. In the FACS experiments conducted, the pre-sort fractions always had more DNA than the post-sort fraction, most likely because of the presence of eDNA and the fact that during the sorting process eDNA is likely dissociated from the cells. Thus the presence of eDNA, which could be the result of cellular apoptosis and/or bodily fluid secretions, may be a factor in a successful FACS separation (33).

The impact of one or more of the previously mentioned factors on the epithelial skin cells used in this study could explain unexpected antibody binding results, as well as the variability across individuals using the same antibody. Despite this, the optimization of hormone antibodies using epithelial skin cells was able to be conducted due to reproducible differences in the antibody staining signatures. The overall purpose of this study was to determine if it was possible to facilitate separation between the male and female cell populations, which was deemed possible.

Conclusion

1. Conclusions of the Research

The results from this study show that male and female trace epithelial cells can be stained by targeting testosterone, dihydrotestosterone, and estradiol sex hormones within cell populations and differentiated by flow cytometry. Anti-testosterone and anti-estradiol staining of epithelial cells yields a significant difference when compared to unstained cells, as well as between male and female cell populations. The same cannot be said of anti-DHT or anti-DHT paired with anti-testosterone.

More research is needed in order to determine if trace epithelial cell mixtures can be simplified prior to DNA profiling by targeting testosterone and estradiol sex hormones within cell

populations followed with FACS sorting to separate populations. However, this study shows promising results for optimizing sex hormone antibodies, DNA staining, and targeting cells with nuclei in software programs.

2. Impact

Using Alexa 488-conjugated anti-testosterone, FITC-conjugated anti-DHT, Alexa 647-conjugated anti-estradiol, and Alexa 647-conjugated anti-testosterone antibodies as fluorescent tags to screen for male epithelial cells is an innovative concept that could benefit forensic biology units with casework. Preferential labeling of male cells can be utilized for screening at crime scenes and in the lab to identify where male cells, and presumably male DNA, are present on evidence. However, in order to develop a screening tool, preferential or sufficiently different (from females) labeling of male cells must be conclusively demonstrated. Flow cytometry was used as a tool for determining if preferential labeling of male cells could be achieved with the additional benefit of cell mixture simplification prior to DNA analysis. Mixture simplification prior to DNA analysis would have a major impact not only in creating DNA mixtures which are easier to interpret, but also post-sort fractions which provide greater statistical power given enhancement for contributors in the different fractions. Overall, insights generated from this technique will contribute to the improvement of forensic science and our understanding of epithelial skin cell evidence in particular. This in turn, may influence DNA sampling on evidence items which could result in the production of higher quality DNA profiles.

3. Future Directions

3.1. Fluorescence Activated Cell Sorting (FACS)

A major goal of this study was to couple protocols for antibody staining to Fluorescence Activated Cell Sorting (FACS). The purpose of performing FACS was to physically isolate cell

populations prior to DNA profiling and demonstrate that touch mixtures can be resolved using this approach. Isolation of cells was possible with antibody staining, which could help differentiate between male and female cell populations in a mixture. However, after three attempts at FACS, resolving mixtures of male and female DNA was not possible because of insufficient material used for running through the FACS. Further research will need to be performed in order to optimize the protocol for antibody staining to FACS in order to minimize DNA loss and increase reproducibility.

3.2. DNA Staining with GelGreen® and Antibody Hybridization

It was expected that the GelGreen® would fluoresce in the green channel while the Alexa 647 anti-testosterone antibody would fluoresce in the red channel. However, this was not the case as the antibody did not fluoresce at all. More experimentation will need to be done with the DNA staining experiment in order to determine the best way to effectively combine the two protocols.

References

1. Kanokwongnuwut, P., Kirkbride, L. P., & Linacre. A. Detection of latent DNA. Forensic Science International: Genetics 2018, 37(1): 95-101.
2. Mozayani, A., Noziglia, C. The Forensic Laboratory Handbook Procedures and Practice. New York City, New York: Humana Press 2011, 18-19.
3. Gaensslen, R. E. Sourcebook in Forensic Serology, Immunology, and Biochemistry. Washington D.C.: U.S. Department of Justice 1983, 101-116.
4. Lincoln, C. E., McBride, P. M., Turbett, G. R., Garbin, C. D., & MacDonald, E. J. The use of an alternative light source to detect semen in clinical forensic medical practice. Journal of Clinical Forensic Medicine 2006, 13(4): 215-218.
5. Thorogate, R., Moreira, J. C. S., Jickells, S., Miele, M. M. P., & Daniel, B. A novel fluorescence-based method in forensic science for the detection of blood in situ. Forensic Science International: Genetics 2008, 2: 363-371.
6. Kanokwongnuwut, P., Martin, B., Kirkbride, K. P., & Linacre, A. Shedding light on shedders. Forensic Science International: Genetics 2018, 36(1), 20-25.
7. Wolkowicz, R. Fluorescence-Activated Cell Sorting. Brenner's Encyclopedia of Genetics 2013, 80-82.
8. Valeggia, C., Nũnez de-la Mora, A. Human Reproductive Ecology 2015, 295-308.
9. Stroud, L. R., Solomon, C., Shenassa, E., Papandonatos, G., Niaura, R., Lipsitt, L. P., LeWinn, K., & Buka, S. L. Long-term stability of maternal prenatal steroid hormones from the National Collaborative Perinatal Project: Still valid after all these years. Psychoneuroendocrinology 2007, 32(2): 140-150.

10. Weisz, J., Ward, I. L. Plasma Testosterone and Progesterone Titers of Pregnant Rats, Their Male and Female Fetuses, and Neonatal Offspring. Endocrinology 1980, 106: 306-316.
11. Chen, H. C., Farese, Jr. R.V. Steroid hormones: Interactions with membrane-bound receptors. Current Biology 1999, 9(13): R478-R481.
12. Atkins, P. W. Molecules. 1987. New York: W. H. Freeman.
13. Hoberman, J. M., Yesalis, C. E. The History of Synthetic Testosterone. Scientific American 1995, 272: 76–82.
14. Marchetti, P. M., & Barth, J. H. Clinical biochemistry of dihydrotestosterone. Annals of Clinical Biochemistry 2013, 50(2): 95–107.
15. Grino, P. B., Griffin, J. E., & Wilson, J. D. Testosterone at high concentrations interacts with the human androgen receptor similarly to dihydrotestosterone, Endocrinology 1990, 126: 1165-1172.
16. Gottlieb, B., Lombroso, R., Beital, L. K., Trifiro, M. A. Molecular pathology of the androgen receptor in male (in)fertility. Reproductive BioMedicine Online 2004, 10(1): 42-48.
17. Lewis, J. G. Steroid Analysis in Saliva: An overview. The Clinical Biochemist Reviews 2006, 27: 139-146.
18. Miller, J. M., Brocato, E. R., Greenspoon, S. A., & Ehrhardt, E. J. Simplification of Epithelial Cell Mixtures through Hormone-specific Antibody Probes and High Throughput Cell Separation. Manuscript in preparation.

19. Nóbrega, L. H. C., Azevedo, G. D., Lima, J. G., Ferriani, R. A., Spritzer, P. M., Sá, T. M. O., & Maranhão. Analysis of testosterone pulsatility in women with ovulatory menstrual cycles, Arq. Bras. Endocrinol. Metab. 2009, 53(8).
20. Voigt, W., Fernandez, E. P., & Hsia, S. L. Transformation of Testosterone into 17beta-Hydroxyalpha-androstan3-one by Microsomal Preparations of Human Skin*. The Journal of Biological Chemistry 1970, 245(21): 5594-5599.
21. van Oorschot, R. A., Ballantyne, K. N., & Mitchell, R. J. Forensic trace DNA: a review. Investigative genetics 2010, 1(1), 14.
22. Department of Forensic Science Manuals and Procedures website. https://www.dfs.virginia.gov/documentation-publications/manuals/.
23. Philpott, M. K., Stanciu, C. E., Kwon, Y. J., Bustamante, E. E., Greenspoon, S. A., & Ehrhardt, C. J. Analysis of cellular autofluorescence in touch samples by flow cytometry: implications for front end separation of trace mixture evidence. Analytical and Bioanalytical Chemistry 2017, 409(17), 4167–4179.
24. Sowers, M. F., Beebe, J. L., McConnell, D., Randolph, J., & Jannausch, N. Testosterone concentrations in women aged 25–50 years: Associations with lifestyle, body composition, and ovarian status, Am. J. Epidemiol. 2001, 153(3): 256-264.
25. Travison, T. G., Vesper, H. W., Orwoll, E., Wu, F., Kaufman, J. M., Wang, Y, & Bhasin, S. Harmonized reference ranges for circulating testosterone levels in men of four cohort studies in the United States and Europe, The Journal of Clinical Endocrinology & Metabolism 2017, 102(4): 1161–1173.
26. Nieschlag, E., Behre, H. M., & Nieschlag, S. Testosterone: Action, Deficiency, Substitution. Cambridge University Press 2012, 4: 494-497.

27. Wiznia, L. E., & Elbuluk, N. Differences in Skin Structure and Function in Ethnic Populations. Dermatoanthropology of Ethnic Skin and Hair 2017: 35–48.
28. Rognoni, E., Watt, F. M. Skin Cell Heterogeneity in Development, Wound Healing, and Cancer, Trends Cell Biol. 2018, 28(9): 709-722.
29. Sandby-Moller, J., Poulsen, T., Wulf, H. C. Epidermal thickness at different body sites: Relationship to age, gender, pigmentation, blood content, skin type and smoking habits, Acta. Derm. Venereo 2003, 83: 410–413.
30. Nakamura, K., Ito, Y., Matsumoto, K., Daikoku, E., Kiyokane, K., & Otsuki, Y. The Relationship between Apoptosis and Keratinization in Human Epidermis. Acta Histochemica Et Cytochemica 1999, 32(1), 77–83.
31. Vandewoestyne, M., Van Hoofstat, D., Franssen A, et al. Presence and potential of cell free DNA in different types of forensic samples. Forensic Sci Int Genet. 2013, 7(2): 316–20.
32. Stanciu, C. E., Philpott, M. K., Kwon, Y. J., Bustamante, E. E., & Ehrhardt, C. J. Optical characterization of epidermal cells and their relationship to DNA recovery from touch samples. F1000Research 2015, 4, 1360.
33. Quinones, I., & Daniel, B. Cell free DNA as a component of forensic evidence recovered from touched surfaces. Forensic Science International: Genetics 2012, 6(1), 26–30.

Critical Data: Tables

Table 1. Mean Intensity, Max Pixel, and Bright Detail Intensity Values of Anti-Testosterone.

	Mean Intensity, Max Pixel, and Bright Detail Intensity Values					
Sample Name	Channels					
	Intensity_MC_Ch02		Max Pixel_MC_Ch02		Bright Detail Intensity R3_MC_Ch02	
	50 mW	150 mW	50 mW	150 mW	50 mW	150 mW
Male S19 0 Testosterone	8.57E+04	1.58E+05	5.45E+01	1.12E+02	6.62E+03	7.72E+03
Male S19 2.5 Testosterone	2.33E+05	4.74E+05	1.55E+02	2.99E+02	8.53E+03	1.32E+04
Female N17 0 Testosterone	1.14E+05	1.24E+05	1.82E+02	2.07E+02	7.19E+03	1.19E+04
Female N17 2.5 Testosterone	1.71E+05	3.75E+05	3.17E+02	7.73E+02	1.43E+04	4.76E+04

Data compares laser powers and conditions in the AMNIS® laser power experiment.

Table 2. Mean Intensity, Max Pixel, and Bright Detail Intensity Values of Anti-Estradiol.

	Mean Intensity, Max Pixel, and Bright Detail Intensity Values					
Sample Name	Channels					
	Intensity_MC_Ch05		Max Pixel_MC_Ch05		Bright Detail Intensity R3_MC_Ch05	
	50 mW	150 mW	50 mW	150 mW	50 mW	150 mW
Male E19 0 Estradiol	7.69E+04	8.51E+04	3.95E+01	5.62E+01	1.08E+04	1.20E+04
Male E19 2.5 Estradiol	1.29E+05	2.26E+05	8.06E+01	2.10E+02	1.52E+04	2.96E+04
Female D02 0 Estradiol	9.24E+04	9.99E+04	4.47E+01	5.71E+01	1.48E+04	1.55E+04
Female D02 2.5 Estradiol	1.97E+05	5.03E+05	1.40E+02	4.11E+02	2.19E+04	4.86E+04

Data compares laser powers and conditions in the AMNIS® laser power experiment.

Table 3. Summary of AMNIS® results.

Antibody	Instrument Guava/Canto vs AMNIS	Greater Discrepancy Male & Female (2.5 vs 5 µL)
488 Anti-Testosterone	Guava	5
	AMNIS	5
647 Anti-Estradiol	Canto	2.5
	AMNIS	2.5

Flow cytometry results were compared to imaging flow cytometry results to determine consistency between the two for each antibody.

Table 4. Summarized Ideas® Software Data.

Using Ideas® Software to Target Nucleated Cells		
Mask Name	Number of Cell Events	Includes Target Cells 60 and 127 (Y/N)
Spot(M02, Ch02, Bright, 5.88, 9, 4)	233	Yes
Intensity(M02, Ch02, 250-500)	18	No, just cell 127
Spot(M02, Ch02, Bright, 5.88, 9, 4) And Intensity(M02, Ch02, 250-500)	370	Yes
Spot(M02, Ch02, Bright, 5.88, 9, 4) And Morphology(M02, Ch02)	370	Yes
Component(1, Circularity, Spot(M02, Ch02, Bright, 5.88, 9, 4), Ascending)	77	No, just cell 127

Various masks were compared to determine most effective in isolating cells with potential nuclei.

Table 5. TrueAllele® Casework analysis for Alexa 647 anti-testosterone 1:1 male:female mixture.

	TrueAllele Software Analysis				
	Pre-Sort		P5 Post-Sort (Left)	P6 Post-Sort (Right)	
	log(LR) Values	Contributor Composition	log(LR) Values	log(LR) Values	Contributor Composition
Male	29	94%	INC (<0)	9	50%
Female	INC (1.3)	6%	INC (<0)	INC	50%

The logarithm of the likelihood ratio (log(LR)) values, regarding the statistical support of female and male STR profiles as contributors to the pre-sort mixture, P5 post-sort, and P6 post-sort fraction, are displayed.

Critical Data: Figures

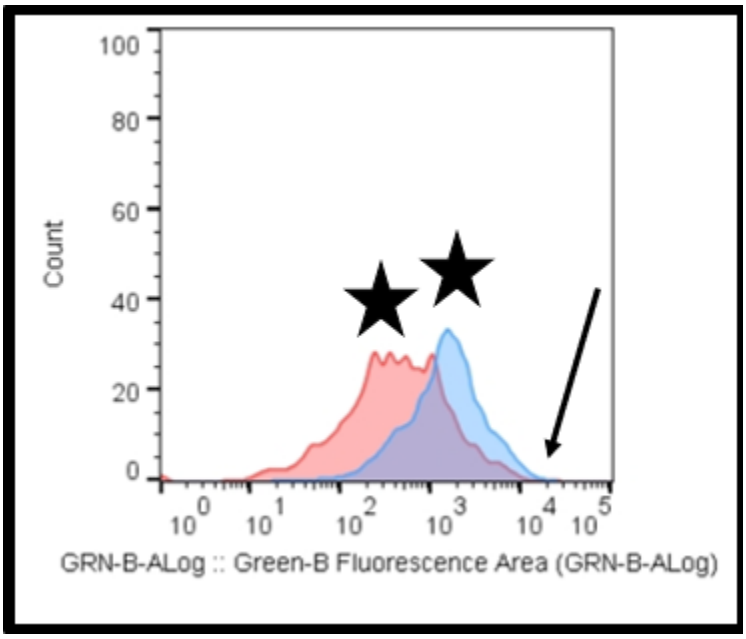

Figure 1. Testing and Comparing Male and Female Cell Subpopulations. The median fluorescence of the male (blue) and female (pink) subpopulations stained with anti-testosterone antibody is indicated by a star. The percent of cells not overlapping at various fluorescence intensities in the histograms as indicated by the arrow can be used to determine if differences in fluorescence exist between male and female fractions.

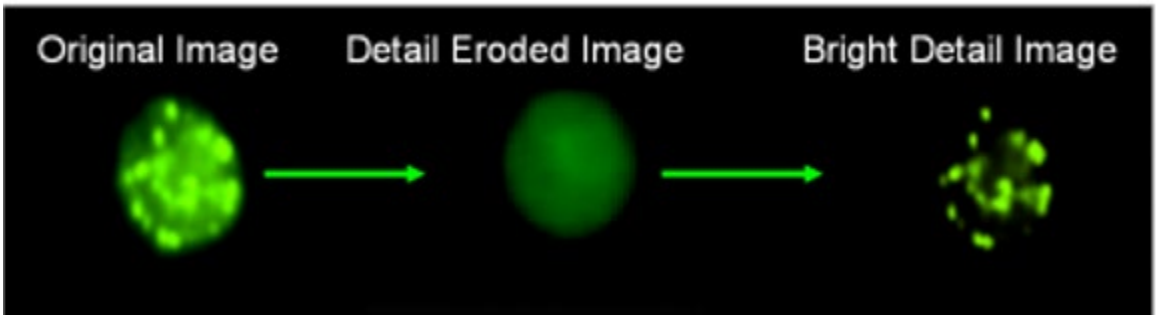

Figure 2. Bright Detail Intensity. Bright detail intensity is defined as the intensity of localized bright spots in the area of the epithelial cell image using the AMNIS® external software program (IDEAS® v. 6.0 Image Data Exploration and Analysis User's Manual, Millipore Inc., Burlington, MA, 2013).

Panel A

	Sample Name	Subset Name	Count
	Female Alexa 10.fcs	Intact Corneocytes	108
	Female Alexa 5.fcs	Intact Corneocytes	40.0
	Female Alexa 2.5.fcs	Intact Corneocytes	48.0
	Female Alexa 0.fcs	Intact Corneocytes	80.0

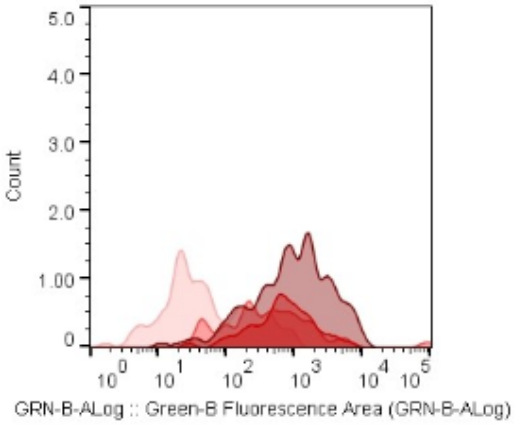

Panel B

	Sample Name	Subset Name	Count
	Male Alexa 10.fcs	Intact Corneocytes	114
	Male Alexa 5.fcs	Intact Corneocytes	37.0
	Male Alexa 2.5.fcs	Intact Corneocytes	38.0
	Male Alexa 0.fcs	Intact Corneocytes	50.0

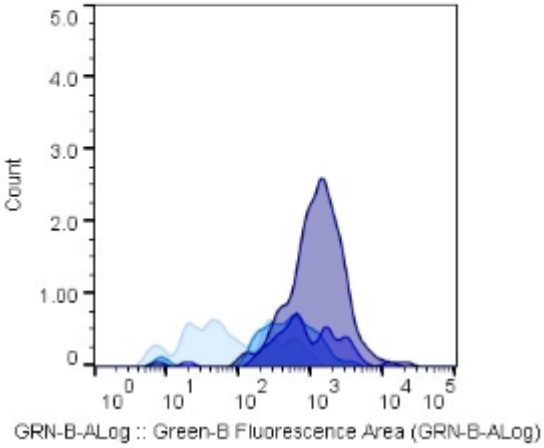

Figure 3. Panel A & Panel B. Testing and Comparing Female and Male Cell Subpopulations Stained with Varying Concentrations of Anti-Testosterone linked to Alexa 488. Female cells are Panel A, male cells are Panel B. These gated histograms represent unstained and stained cells at various anti-testosterone antibody concentrations starting with unstained and proceeding with unstained, 2.5 µL (1.75E-3 µg/µL), 5 µL (3.5E-3 µg/µL), and 10 µL (7.0E-3 µg/µL). These histograms demonstrate if there was a shift from the unstained to stained cells. X-axis is fluorescence intensity, y-axis is cell count.

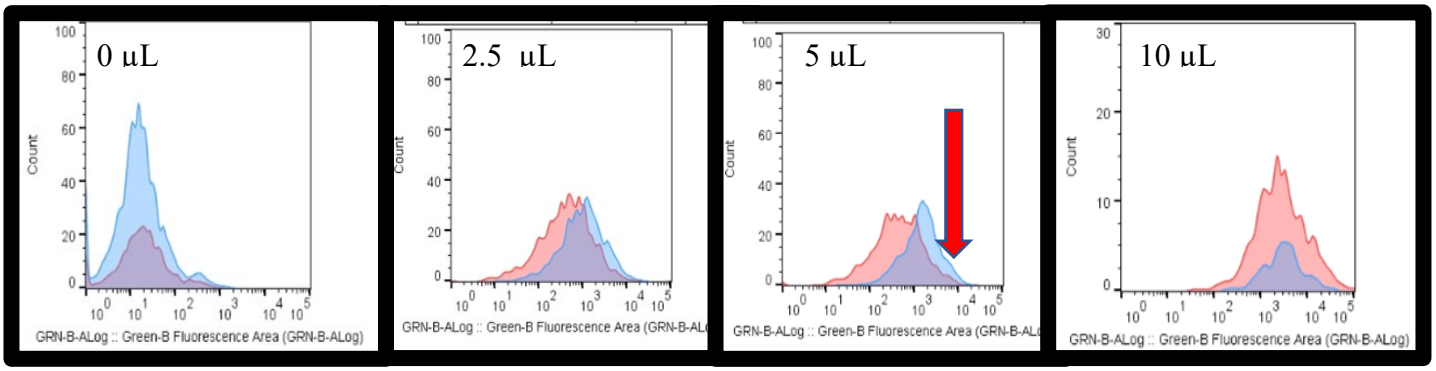

Figure 4. Comparing Male and Female Cell Subpopulations Stained with Varying Concentrations of Anti-Testosterone. The median fluorescence of the male (blue) and female (pink) subpopulations stained with anti-testosterone antibody. Arrow indicates area of nonoverlap.

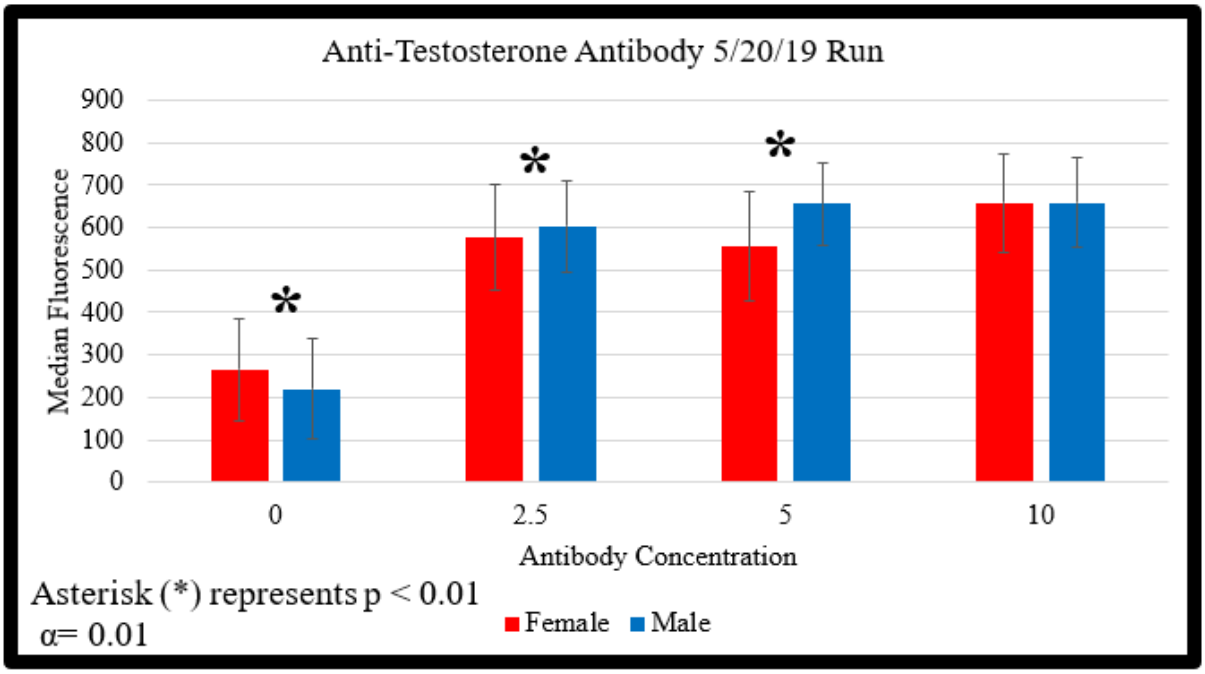

Figure 5. Comparison between male and female cell populations stained with anti-testosterone. Bars represent median fluorescence. Asterisk represents statistical significance when $p < 0.01$ with an alpha of 0.01.

Panel A Panel B

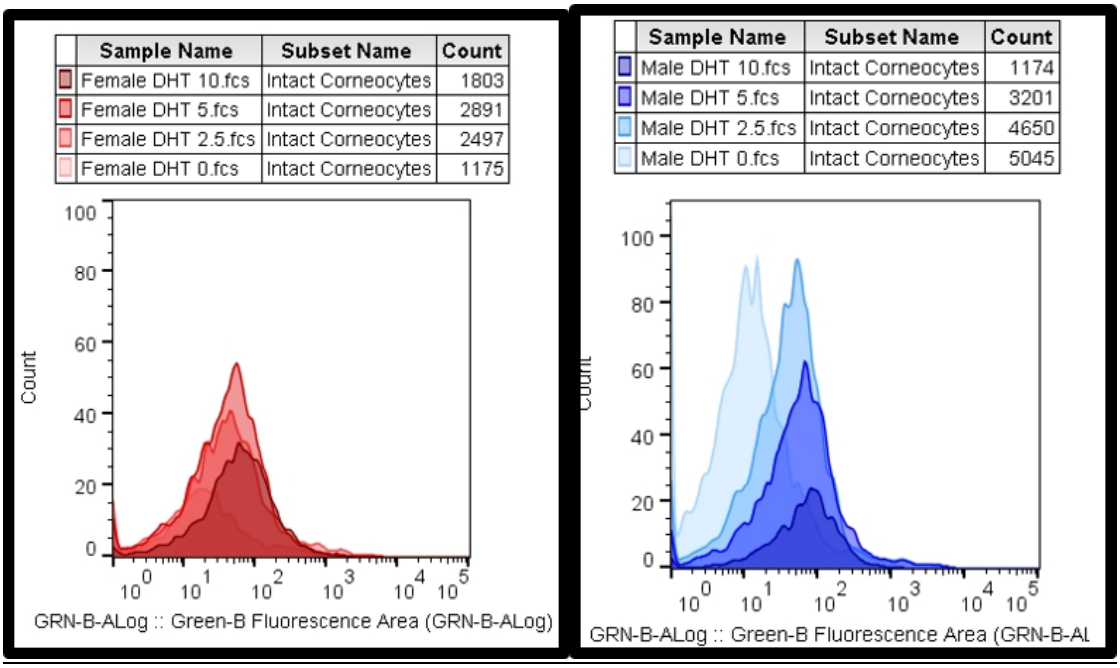

Figure 6. Panel A & Panel B. Testing and Comparing Female and Male Cell Subpopulations Stained with Varying Concentrations of Anti-DHT. Female cells are Panel A, male cells are Panel B. These gated histograms represent unstained and stained cells at various anti-DHT antibody concentrations starting with unstained and proceeding with unstained, 2.5 µL (1.02E-3 µg/µL), 5 µL (2.1E-3 µg/µL), and 10 µL (4.1E-3 µg/µL) . These histograms demonstrate if there was a shift from the unstained to stained cells. X-axis is fluorescence intensity, y-axis is cell count.

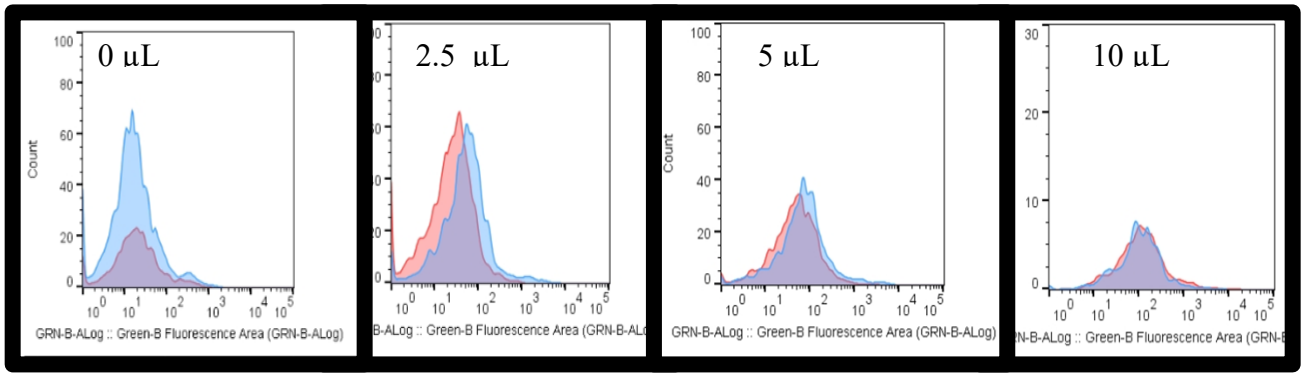

Figure 7. Comparing Male and Female Cell Subpopulations Stained with Varying Concentrations of Anti-DHT. The median fluorescence of the male (blue) and female (pink) subpopulations stained with anti-DHT antibody.

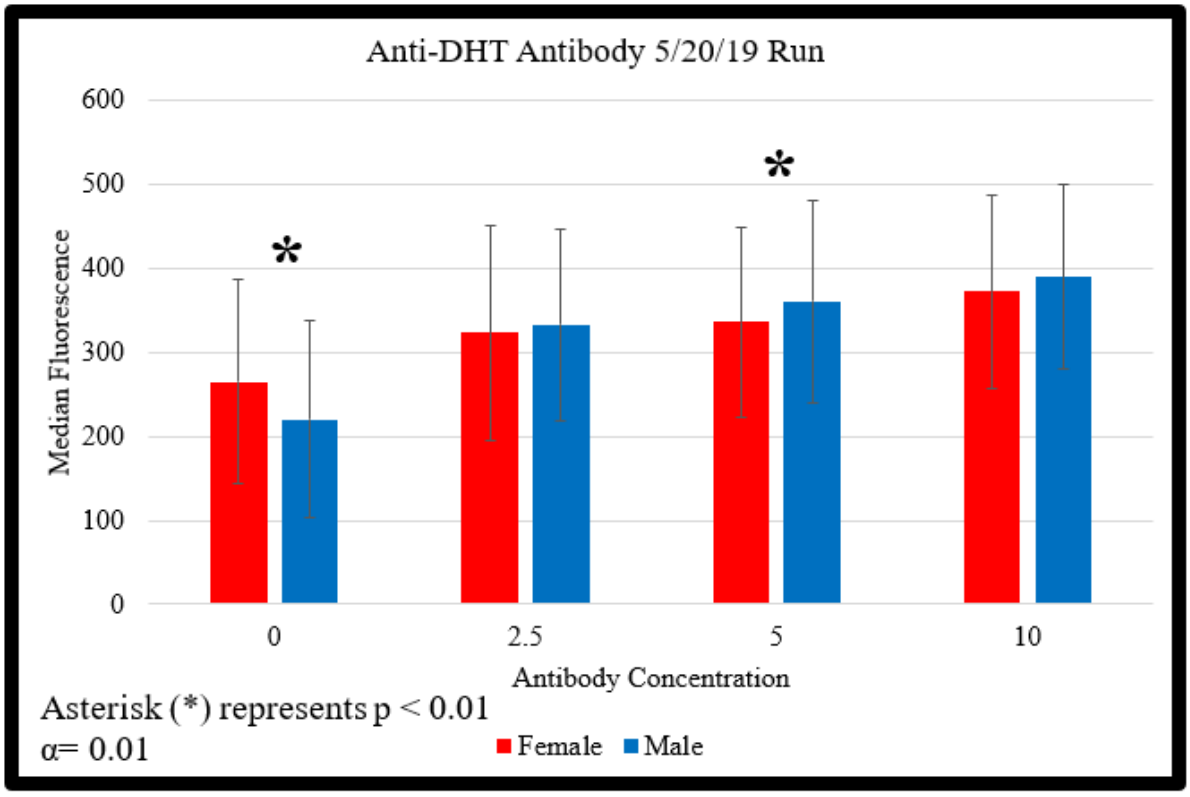

Figure 8. Comparison between male and female cell populations stained with anti-dihydrotestosterone (anti-DHT). Bars represent median fluorescence. Asterisk represents statistical significance when $p < 0.01$ with an alpha of 0.01.

Panel A Panel B

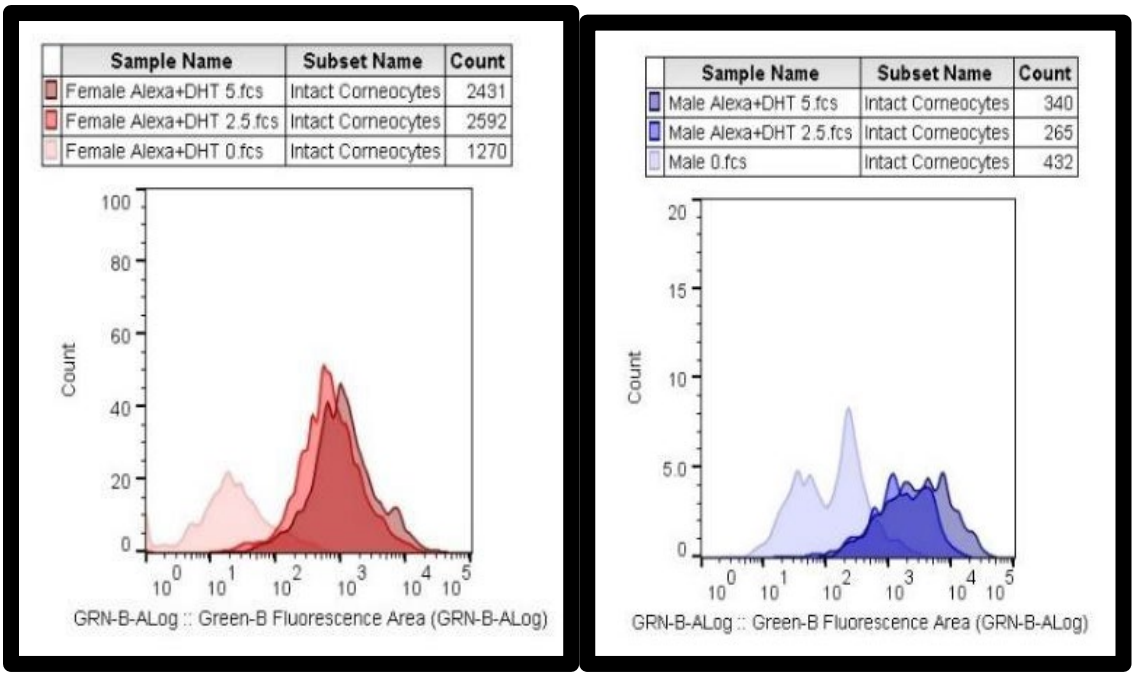

Figure 9. Panel A & Panel B. Testing and Comparing Female and Male Cell Subpopulations Stained with Varying Concentrations of Anti-Testosterone and Anti-DHT. Female cells are Panel A, male cells are Panel B. These gated histograms represent unstained and stained cells at various anti-testosterone and anti-DHT antibody concentrations starting with unstained and proceeding with unstained, 2.5 (2.78E-3 µg), and 5 µL (5.55E-3 µg). These histograms demonstrate if there was a shift from the unstained to stained cells. X-axis is fluorescence intensity and y-axis is cell count.

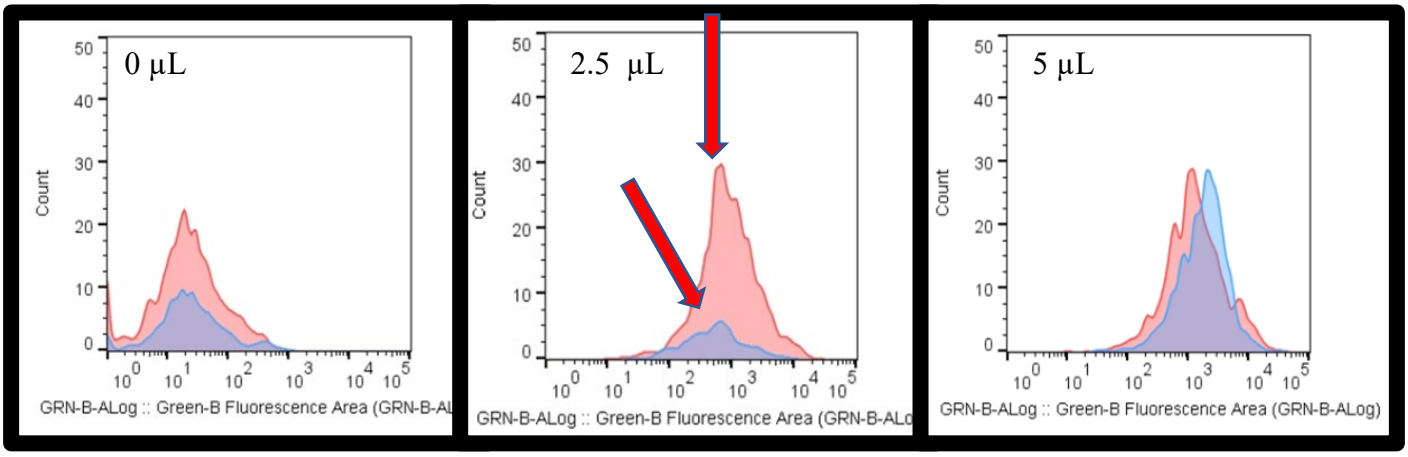

Figure 10. Comparison of male and female cell populations stained with varying concentrations of anti-Testosterone and anti-DHT. The male cells are shown in blue and female in pink. Arrows indicate peaks of female and male cell populations respectively.

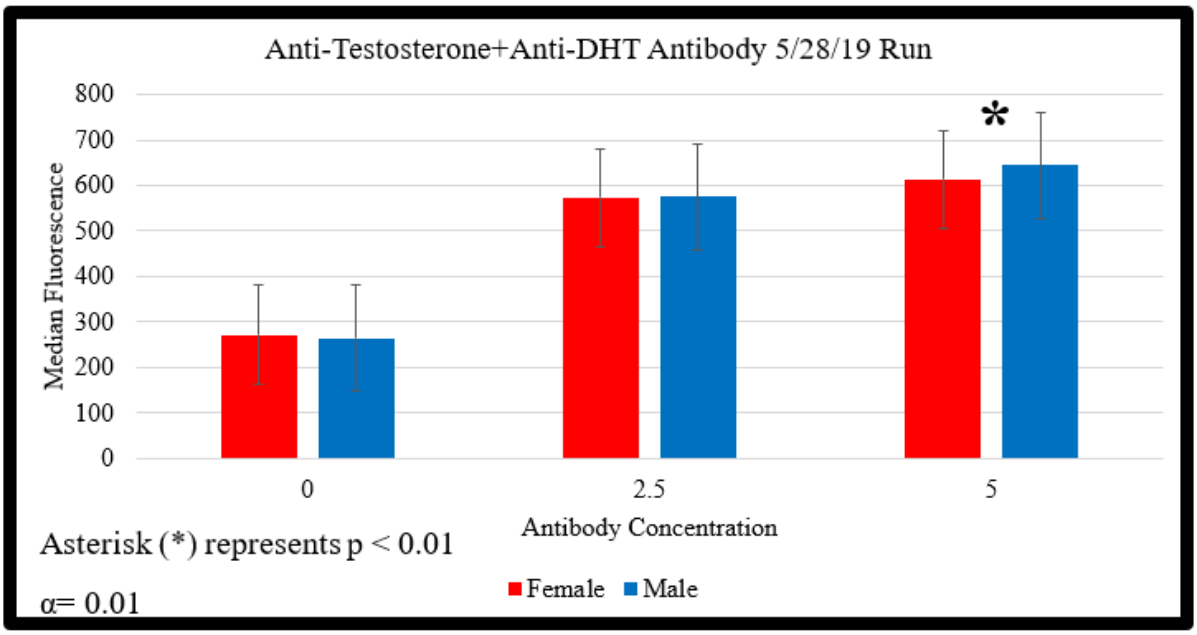

Figure 11. Comparison between male and female cell populations stained with both anti-testosterone and anti-dihydrotestosterone. Bars represent median fluorescence. Asterisk represents statistical significance when $p < 0.01$ with an alpha of 0.01.

Panel A

Panel B

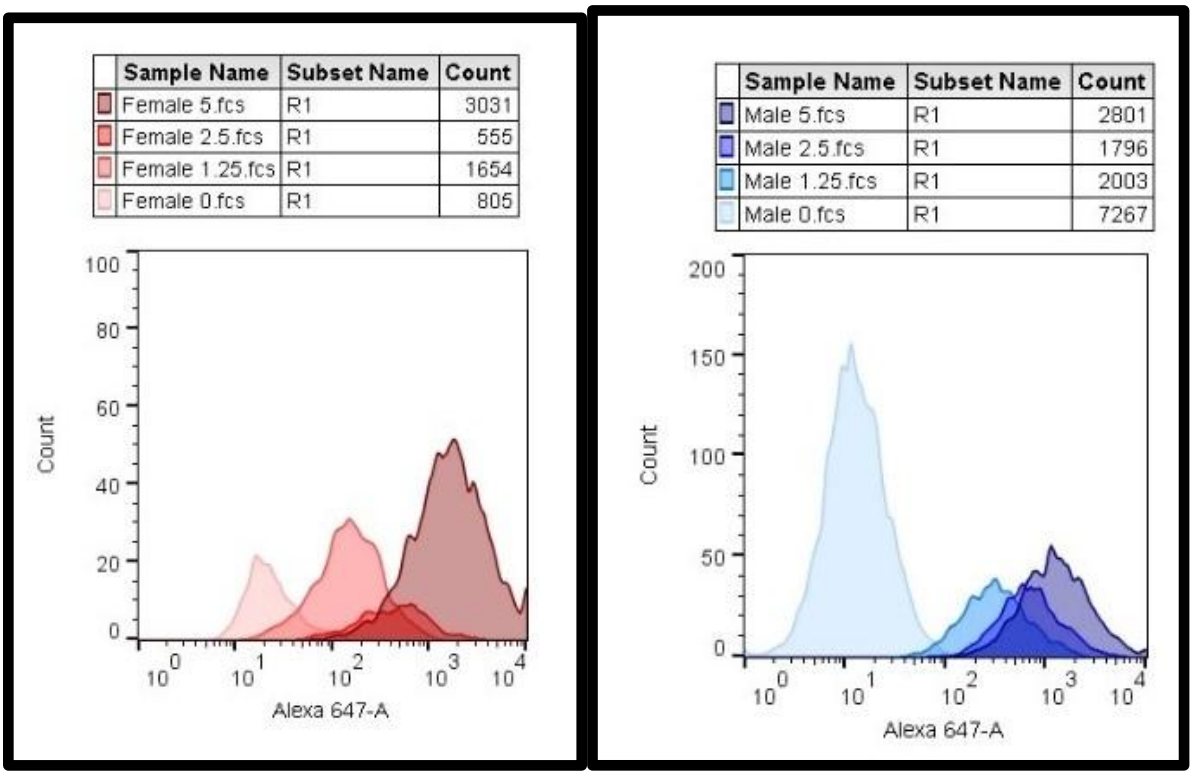

Figure 12. Panel A & Panel B. Testing and Comparing Female and Male Cell Subpopulations Stained with Varying Concentrations of Anti-Estradiol. Female cells are Panel A, male cells are Panel B. These gated histograms represent unstained and stained cells at various anti-estradiol antibody concentrations starting with unstained and proceeding with unstained, 1.25 µL (2.5E-4 µg/µL), 2.5 µL (5.0E-4 µg/µL), and 5 µL (1.0E-3 µg/µL). These histograms demonstrate if there was a shift from the unstained to stained cells. X-axis is fluorescence intensity and y-axis is cell count.

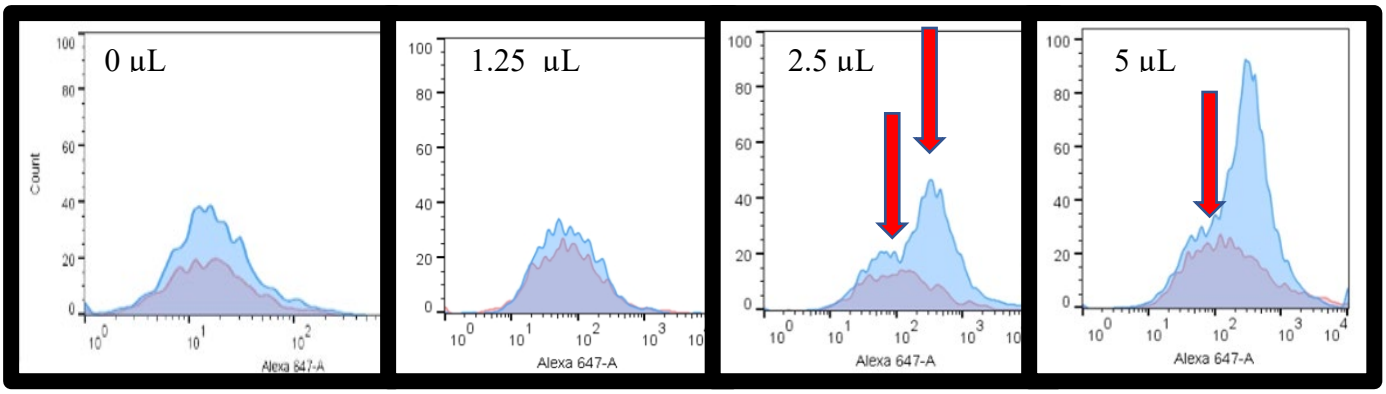

Figure 13. Comparing Male and Female Cell Subpopulations Stained with Varying Concentrations of Anti-Estradiol. The median fluorescence of the male (blue) and female (pink) subpopulations stained with anti-estradiol antibody. Arrows indicate peaks of female and male cell populations respectively.

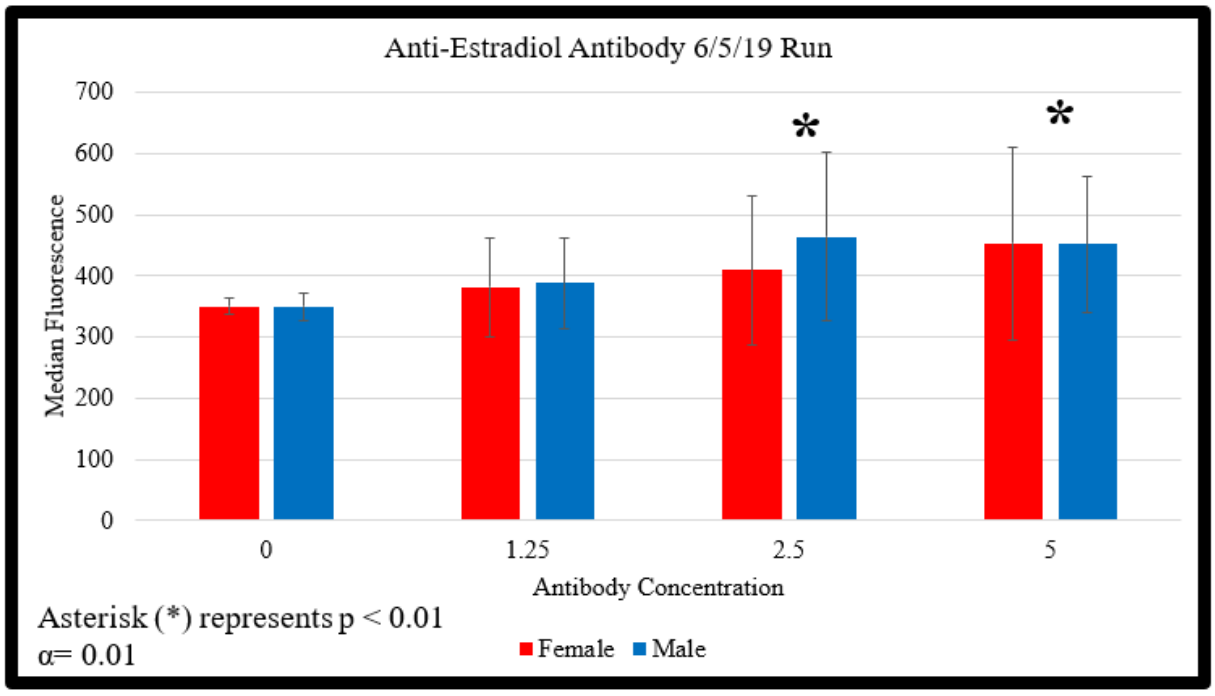

Figure 14. Comparison between male and female cell populations stained with anti-estradiol. Bars represent median fluorescence. Asterisk represents statistical significance when $p < 0.01$ with an alpha of 0.01.

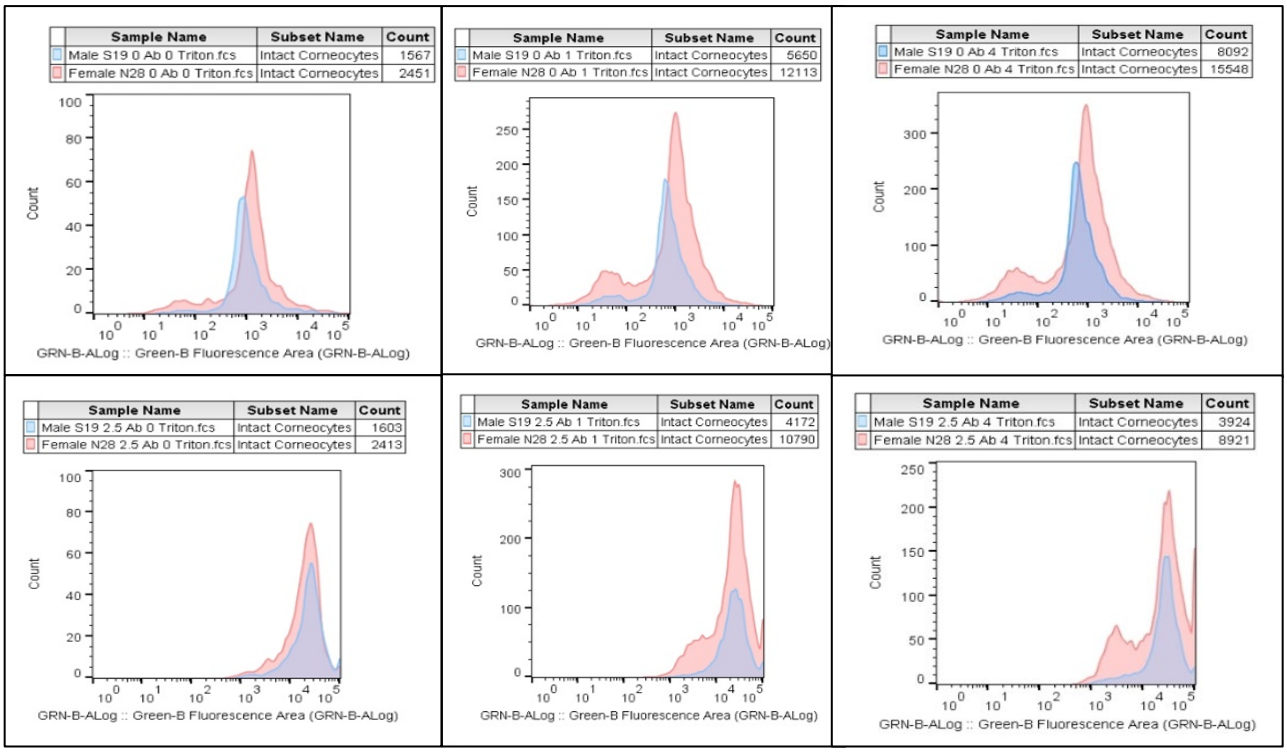

Figure 15. Cell Permeabilization Experiment using Triton-X. The median fluorescence of the male (blue) and female (pink) populations stained with Alexa 488-conjugated anti-testosterone antibody. (Top Row) Comparing Male and Female Cell Subpopulations Stained with Varying Concentrations of Triton-X and 0 Antibody Added (0, 1, and 4 µL). (Bottom Row) Comparing Male and Female Cell Subpopulations Stained with Varying Concentrations of Anti-Testosterone Antibody and Triton-X Added (0, and 2.5 µL (1.02E-3 µg/µL)).

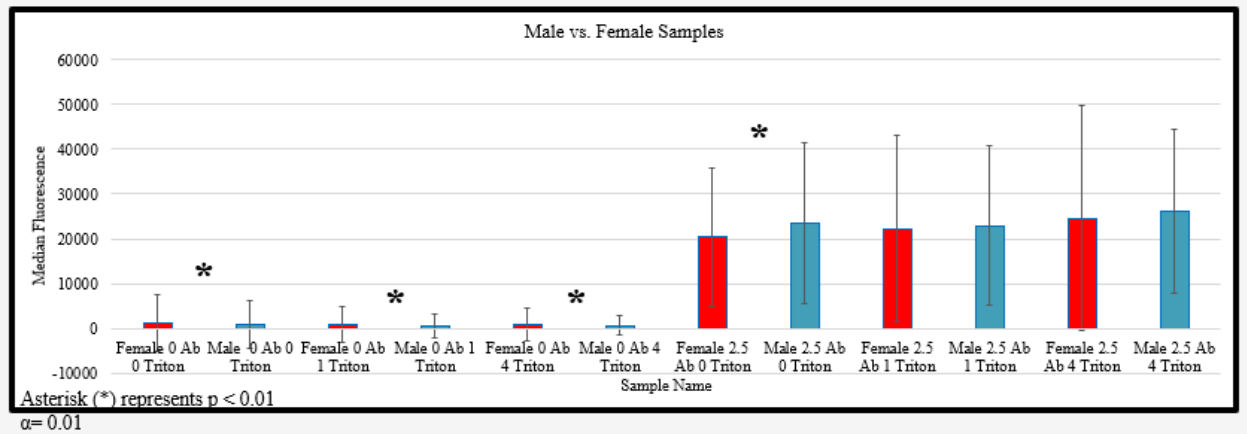

Figure 16. Comparison of the effect of Triton-X 100 cell permeabilization on subsequent staining with anti-testosterone antibody. Male and female cell populations were tested with and without Triton-X 100 (Triton) and with 2.5 µL (1.02E-3 µg/µL) of anti-testosterone. Asterisk represents statistical significance when $p < 0.01$ with an alpha of 0.01.

Panel A

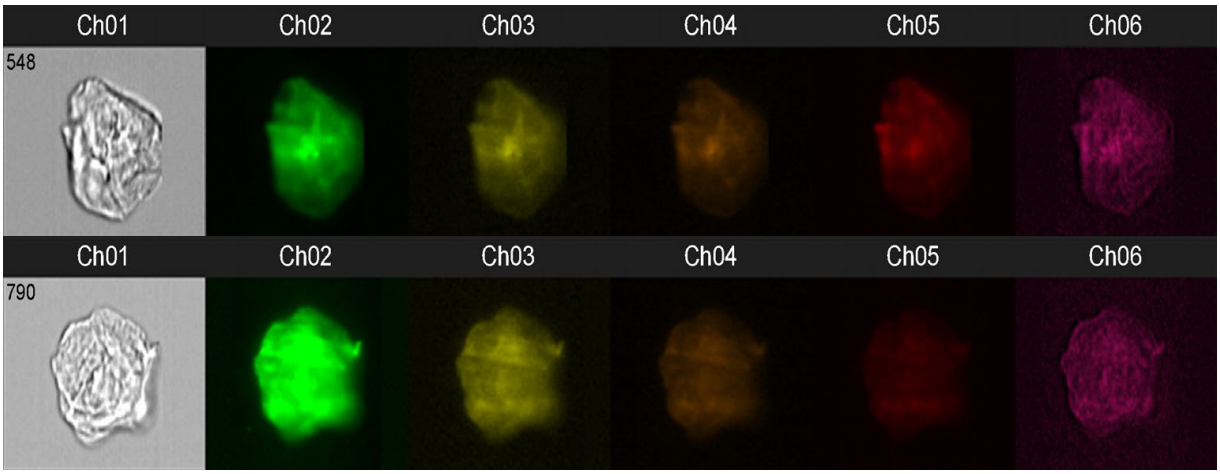

Panel B

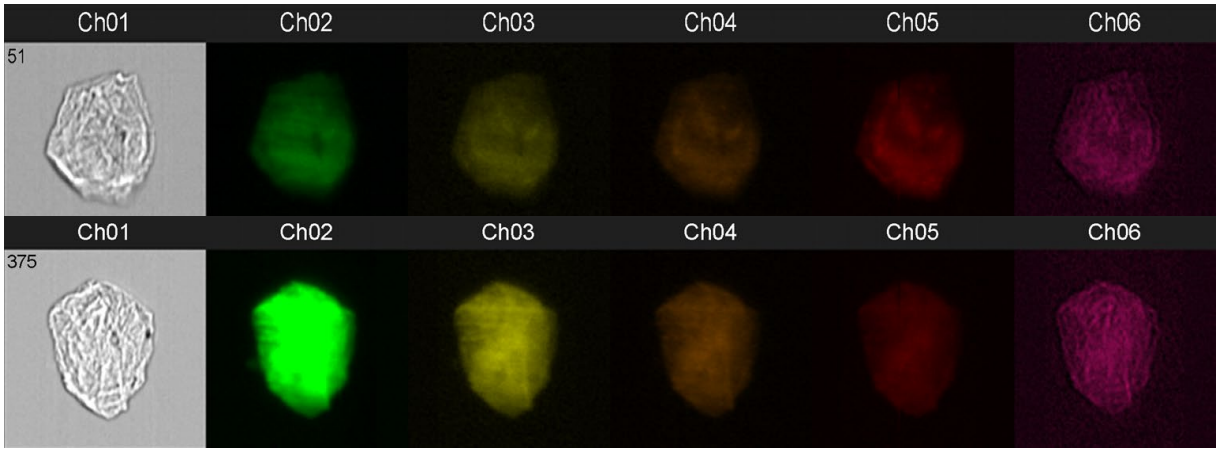

Figure 17. Panel A & Panel B. Anti-Testosterone Female and Male Cells Stained 50 mW (top) vs Stained 150 mW (bottom). Female cells are top two image rows, male cells are bottom two image rows. The same donors were stained with 2.5 µL (1.02E-3 µg/µL) of anti-testosterone and subjected to different laser powers in order to determine which laser power gave the highest data results for Intensity, Max Pixel, and Bright Detail Intensity in Channel 2.

Panel A

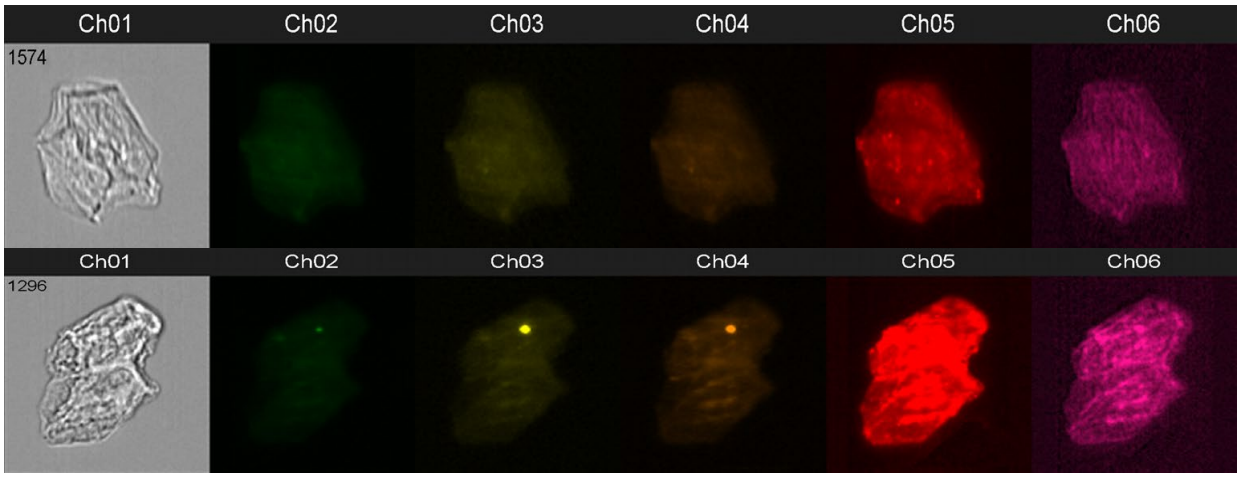

Panel B

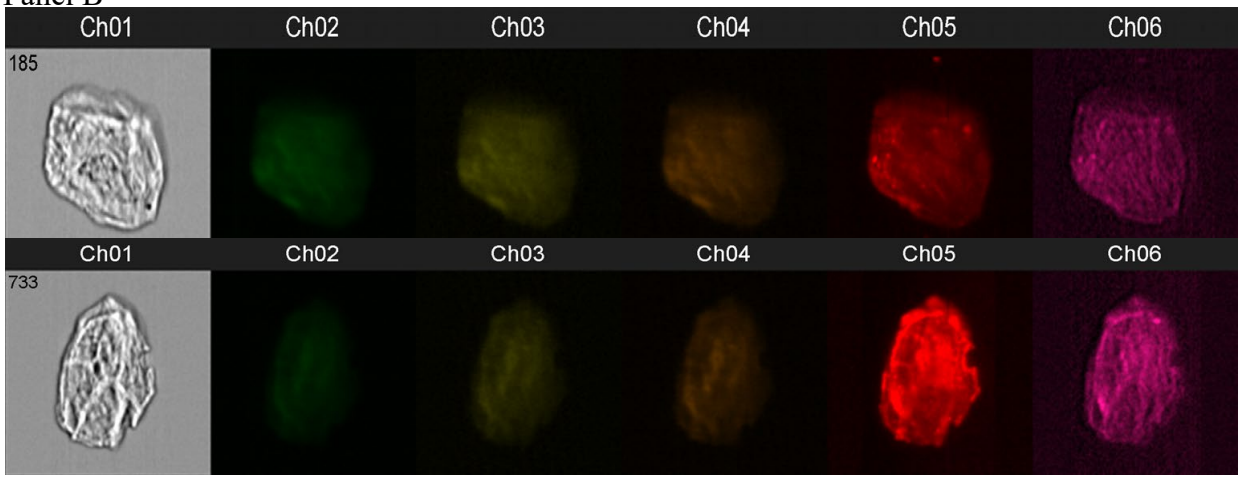

Figure 18. Panel A & Panel B. Anti-Estradiol Female and Male Cells Stained 50 mW (top) vs Stained 150 mW (bottom). Female cells are top two image rows, male cells are bottom two image rows. The same donors were stained with 2.5 µL (5.0E-4 µg/µL) of anti-estradiol and subjected to different laser powers in order to determine which laser power gave the highest data results for Intensity, Max Pixel, and Bright Detail Intensity in Channel 5.

Panel A

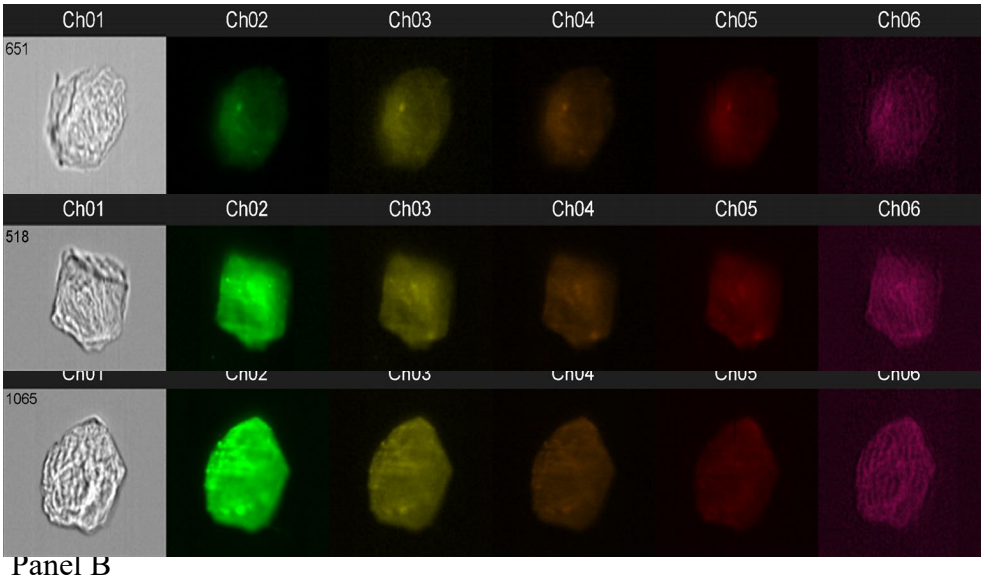

Panel B

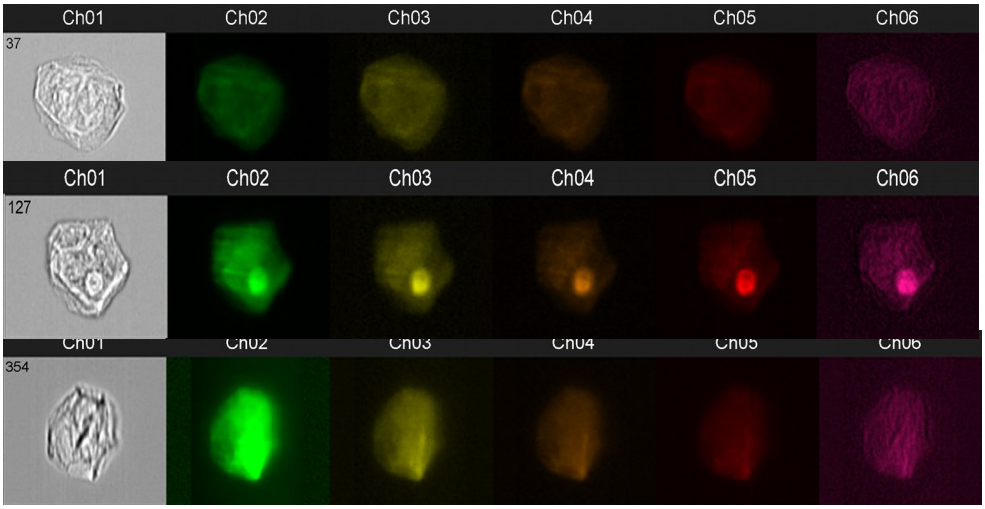

Figure 19. Panel A & Panel B. Anti-Testosterone Female and Male Cells Unstained (top) vs 2.5 Stained (middle) vs 5 Stained (bottom). Female cells are top three image rows, male cells are bottom three image rows. The same donors were stained with various antibody concentrations of 0, 2.5 (1.75E-3 µg/µL), and 5 µL (3.5E-3 µg/µL) of anti-testosterone to determine which antibody concentration gave the highest data results for Intensity, Max Pixel, and Bright Detail Intensity in Channel 2.

Panel A

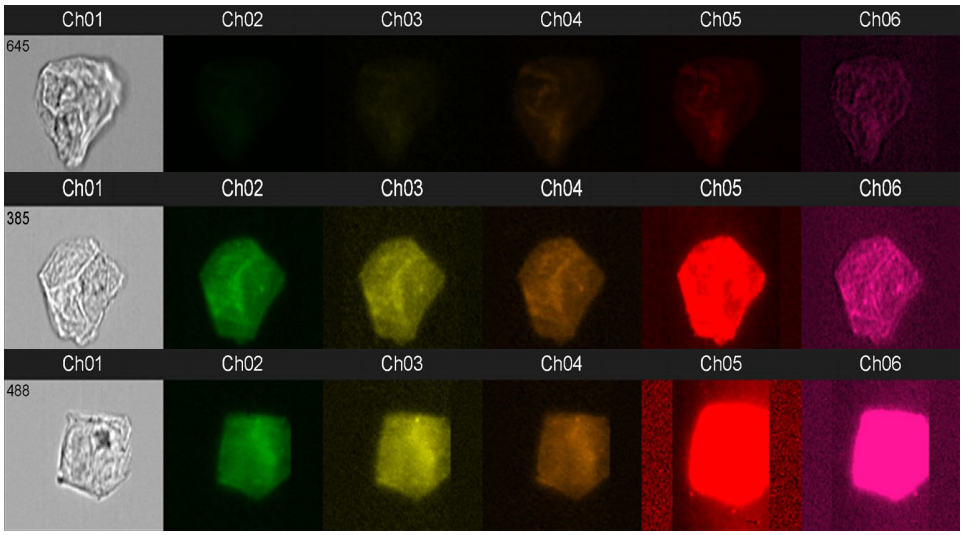

Panel B

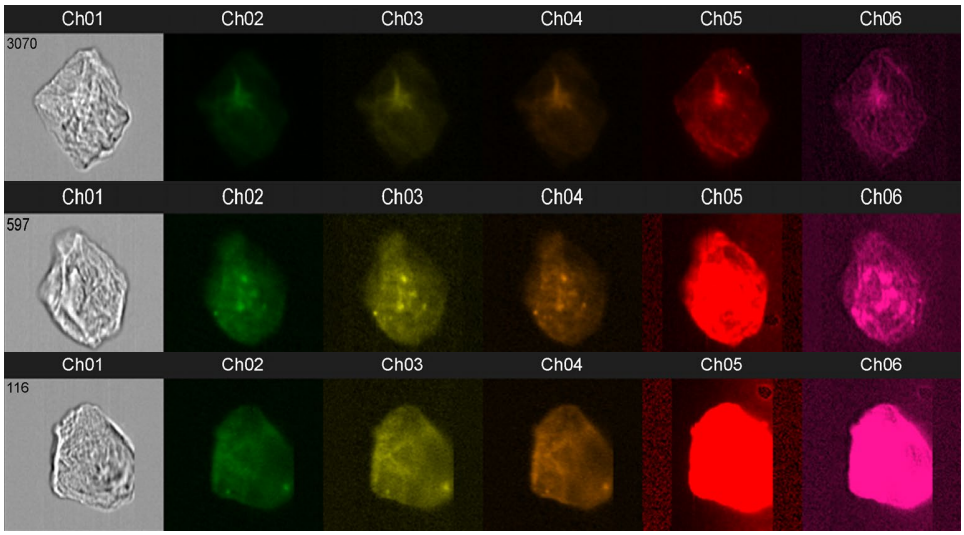

Figure 20. Panel A & Panel B. Anti-Estradiol Female and Male Cells Unstained (top) vs 2.5 Stained (middle) vs 5 Stained (bottom). Female cells are top three image rows, male cells are bottom three image rows. The same donors were stained with various antibody concentrations of 0, 2.5 (5.0E-4 µg/µL), and 5 µL (1.0E-3 µg/µL) of anti-estradiol to determine which antibody concentration gave the highest data results for Intensity, Max Pixel, and Bright Detail Intensity in Channel 5.

Panel A

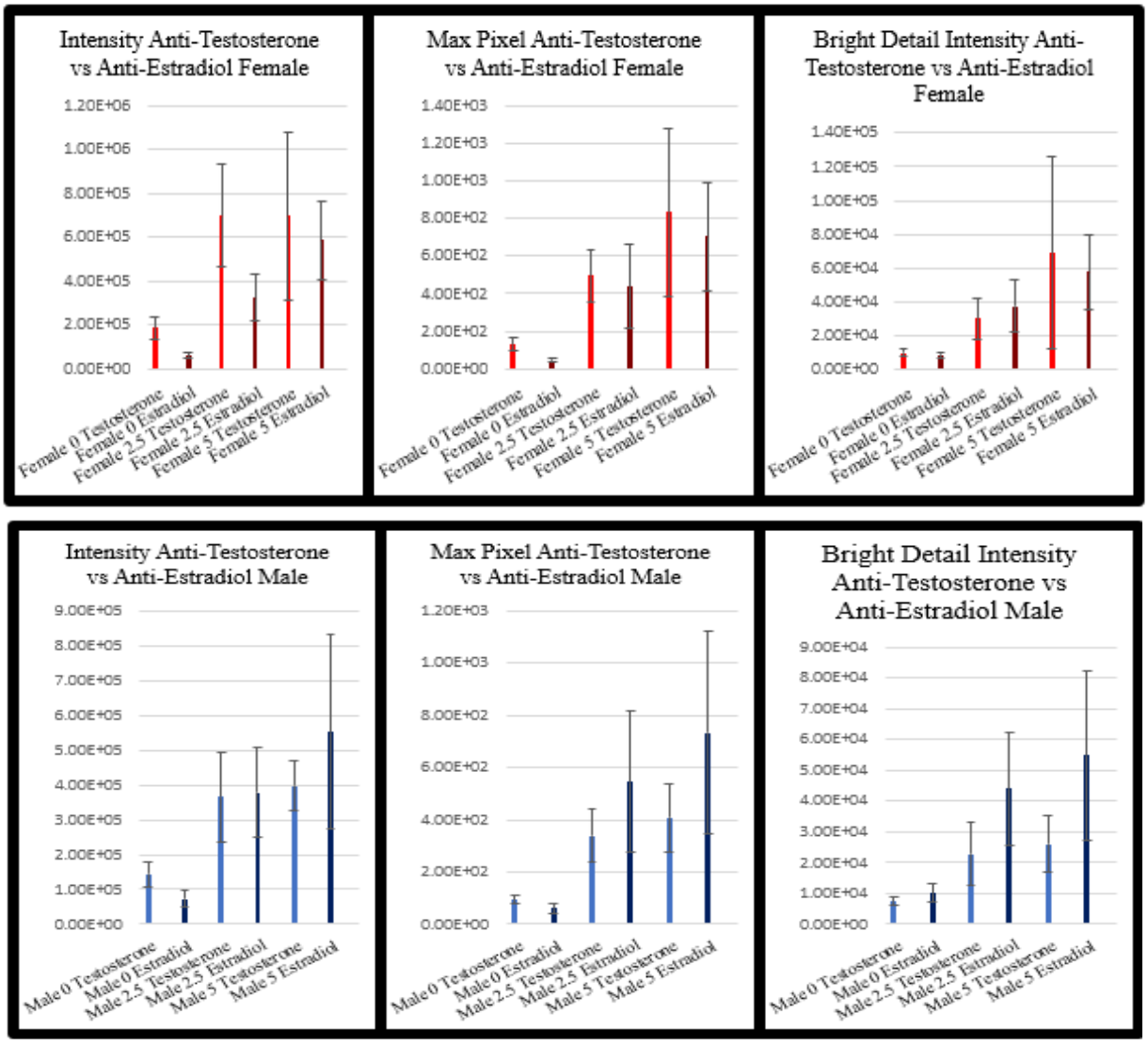

Figure 21. Panel A & Panel B. Anti-Estradiol vs. Anti-Testosterone Female and Male AMNIS® antibody. Female results are top, male results are bottom. Used to determine which antibody has the greater values at the three specified parameters of intensity, max pixel, and bright detail intensity.

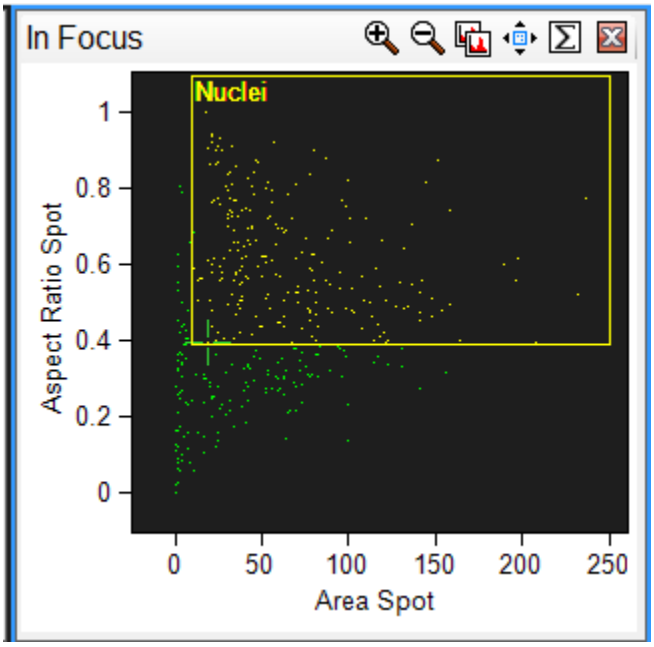

Figure 22. Utilization of the Ideas® Software to Target Nucleated Cells, using the Spot(M02, Ch02, Bright, 5.88, 9, 4) mask. A mask defines a specific area of an image to use for displaying feature-value calculations. The x-axis is the area which represents the number of microns squared in a mask (1 pixel = 0.25 μm^2), the y-axis is the aspect ratio which represents how round or oblong an object is. Green dots represent in-focus large cells and yellow dots represent cells gated for potential nuclei using the mask.

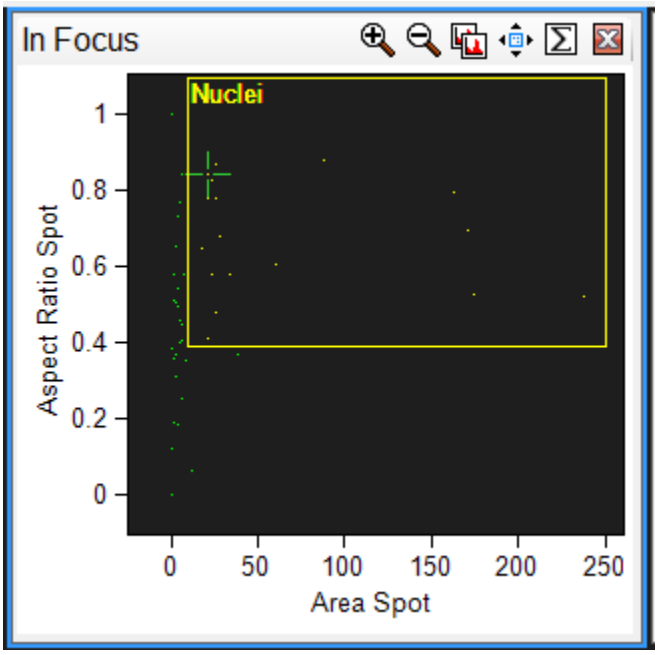

Figure 23. Utilization of the Ideas® Software to Target Nucleated Cells, using the Intensity(M02, Ch02, 250-500) mask. A mask defines a specific area of an image to use for displaying feature-value calculations. The x-axis is the area which represents the number of microns squared in a mask (1 pixel = 0.25 μm^2), the y-axis is aspect ratio which represents how round or oblong an object is. Green dots represent in-focus large cells and yellow dots represent cells gated for potential nuclei using the mask.

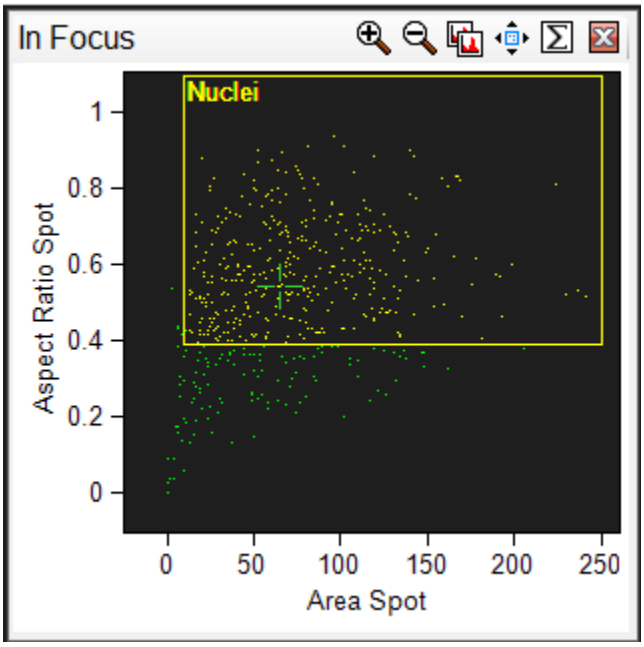

Figure 24. Utilization of the Ideas® Software to Target Nucleated Cells, using the combined Spot(M02, Ch02, Bright, 5.88, 9, 4) And Intensity(M02, Ch02, 250-500) mask. A mask defines a specific area of an image to use for displaying feature-value calculations. The x-axis is the area which represents the number of microns squared in a mask (1 pixel = 0.25 μm^2), the y-axis is aspect ratio which represents how round or oblong an object is. Green dots represent in-focus large cells and yellow dots represent cells gated for potential nuclei using the mask.

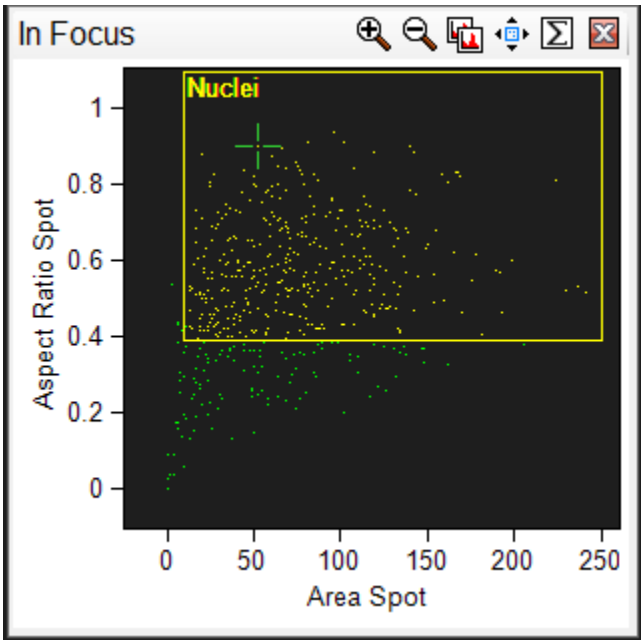

Figure 25. Utilization of the Ideas® Software to Target Nucleated Cells, using the combined Spot(M02, Ch02, Bright, 5.88, 9, 4) And Morphology(M02, Ch02) mask. A mask defines a specific area of an image to use for displaying feature-value calculations. The x-axis is the area which represents the number of microns squared in a mask (1 pixel = 0.25 μm^2), the y-axis is aspect ratio which represents how round or oblong an object is. Green dots represent in-focus large cells and yellow dots represent cells gated for potential nuclei using the mask.

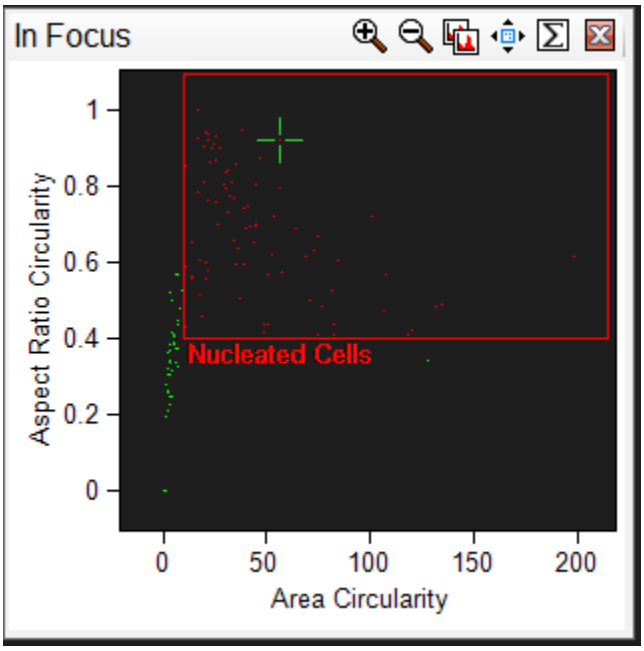

Figure 26. Utilization of the Ideas® Software to Target Nucleated Cells, using the combined Component(1, Circularity, Spot(M02, Ch02, Bright, 5.88, 9, 4), Ascending) mask. A mask defines a specific area of an image to use for displaying feature-value calculations. The x-axis is the area which represents the number of microns squared in a mask (1 pixel = 0.25 μm^2), the y-axis is aspect ratio which represents how round or oblong an object is. Green dots represent in-focus large cells and red dots represent cells gated for potential nuclei using the mask.

Panel A Panel B

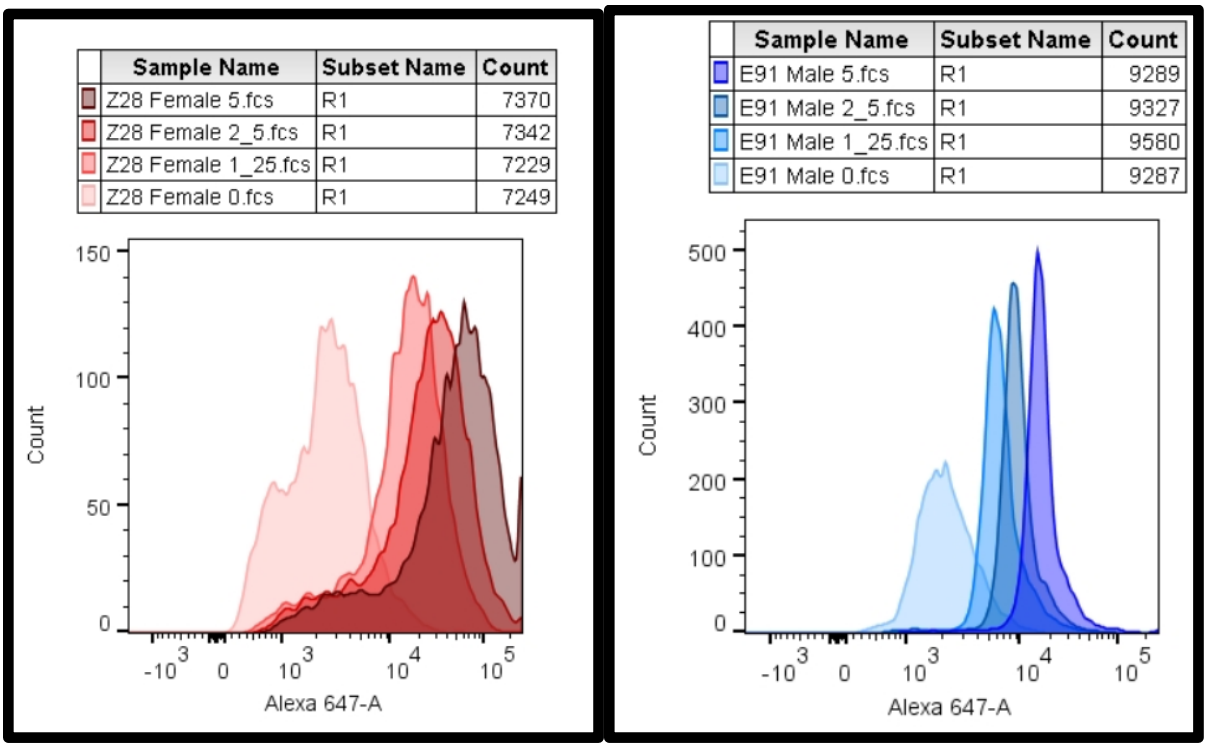

Figure 27. Panel A & Panel B. Testing and Comparing Female and Male Cell Subpopulations Stained with Varying Concentrations of Anti-Testosterone. Female cells are Panel A, male cells are Panel B. These gated histograms represent unstained and stained cells at various anti-testosterone antibody concentrations starting with unstained and proceeding with unstained, 1.25 µL (6.3E-4 µg/µL), 2.5 µL (1.3E-3 µg/µL), and 5 µL (2.5E-3 µg/µL). These histograms demonstrate if there was a shift from the unstained to stained cells. X-axis is fluorescence intensity, y-axis is cell count.

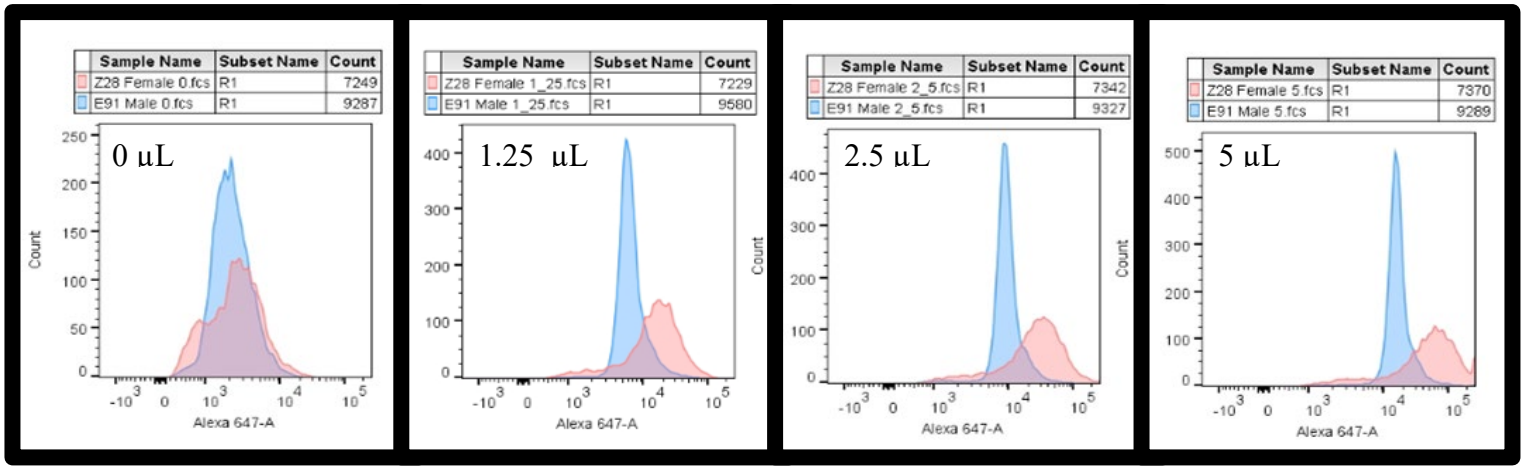

Figure 28. Comparing Male and Female Cell Subpopulations Stained with Varying Concentrations of Anti-Testosterone. The median fluorescence of the male (blue) and female (pink) subpopulations stained with anti-testosterone antibody.

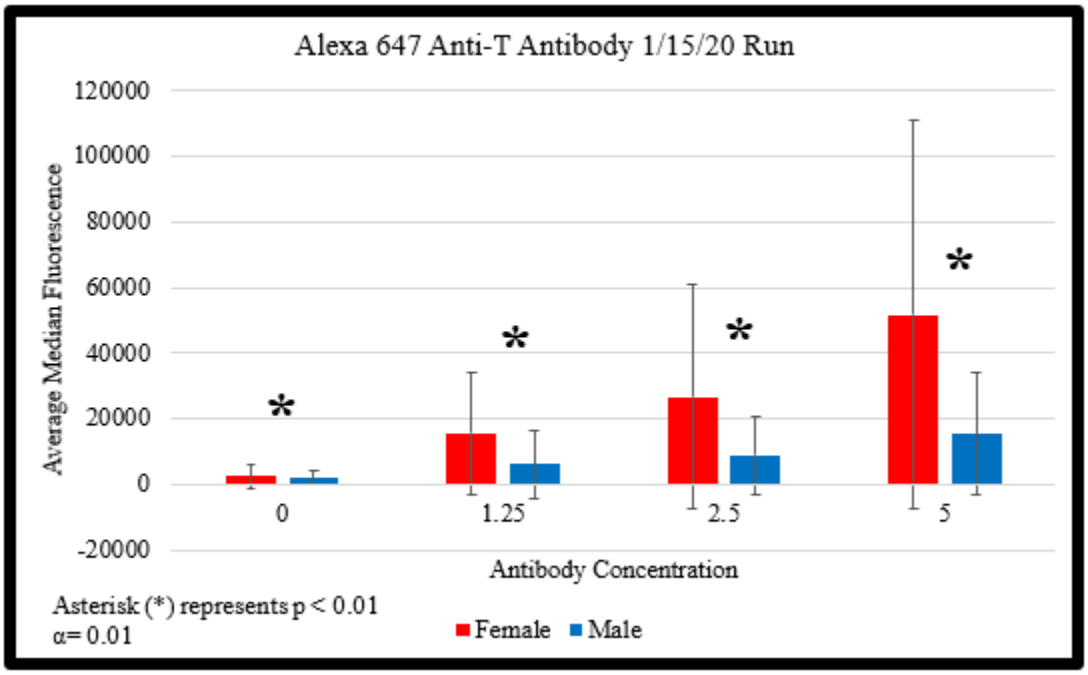

Figure 29. Comparison between male and female cell populations stained with anti-testosterone. Bars represent median fluorescence. Asterisk represents statistical significance when $p < 0.01$ with an alpha of 0.01.

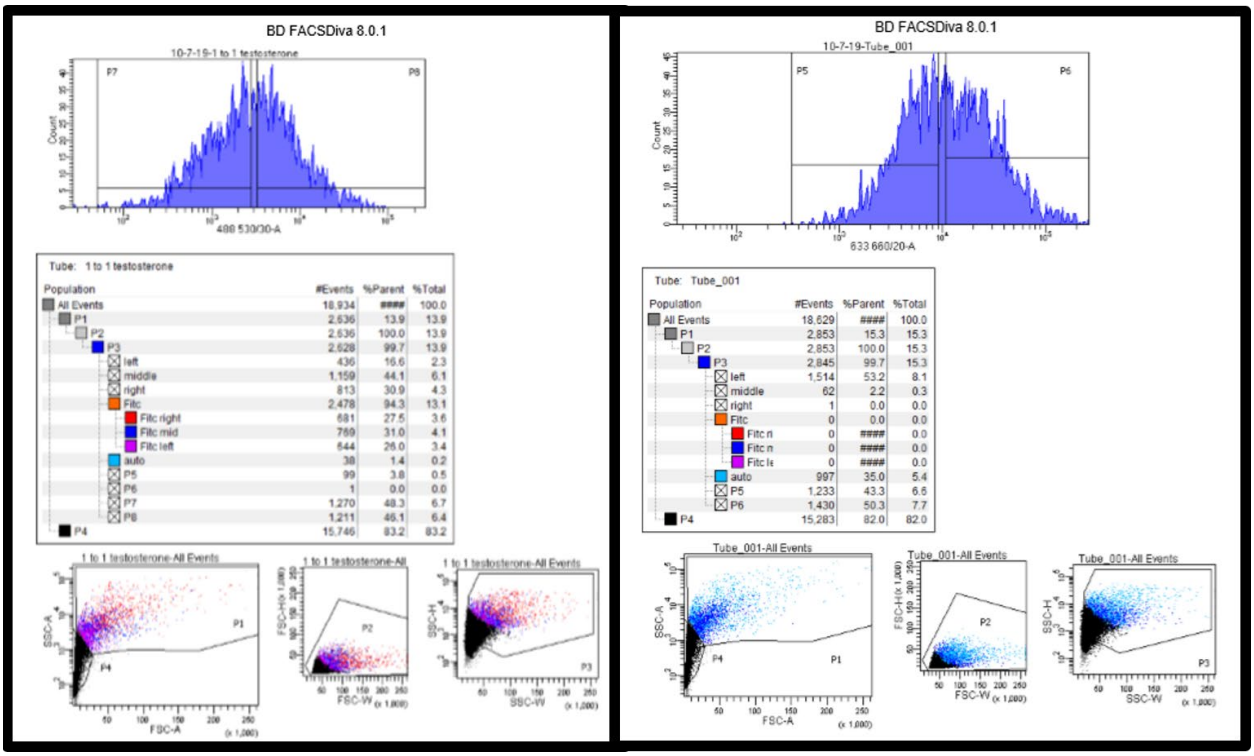

Figure 30. Reports from FACS sorting 1:1 male:female epidermal cell mixtures. Sorting was performed with Alexa 488-conjugated anti-testosterone (left, middle) and Alexa 647-conjugated anti-estradiol (right). Histograms in the reports show little to no separation of 1:1 male:female mixtures in solution.

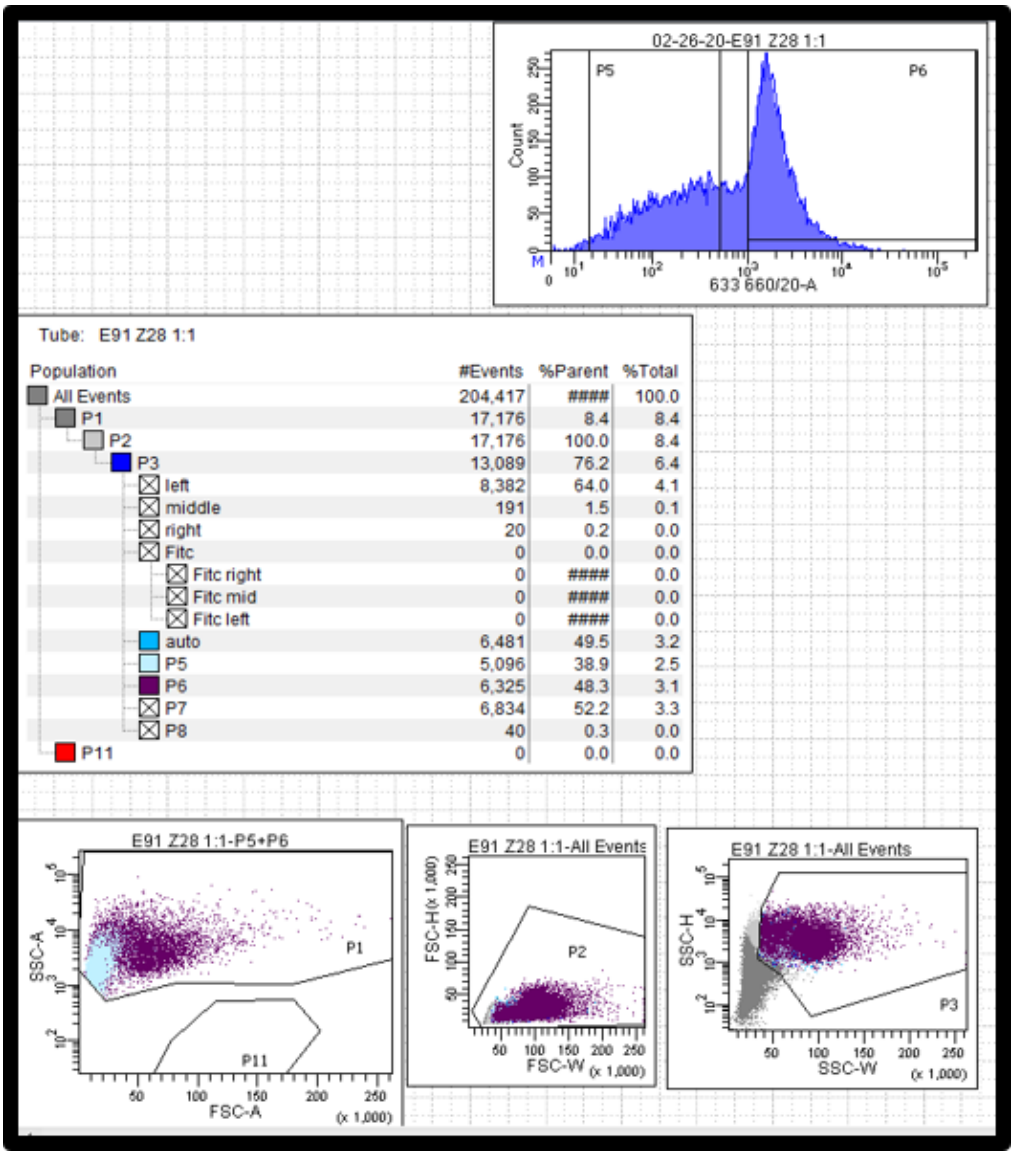

Figure 31. Report from FACS sorting 1:1 male:female mixture with Alexa 647-conjugated anti-testosterone. Histogram in report shows separation of peaks from 1:1 male:female mixture in solution. Plots below the histograms represent the gates for both the P5 and P6 post-sort fractions.

Panel A

	Pre-Sort				
AMEL	**X**	**Y**			
D3S1358	**15**	**(16)**	**18**		
D1S1656	**11**	**(12)**	**14**	**(15)**	**(18.3)***
D2S441	**(10)**	**11**	**14**		
D10S1248	**13**	**14**			
D13S317	**(8)***	**12**			
Penta E	**7**	**(14)**	**15**		
D16S539	**(10)**	**(11)**	**13**	**14**	
D18S51	**(12)**	**14**	**15**		
D2S1338	**17**	**(20)***	**23**		
CSF1PO	**(11)***	**12**	**13**		
Penta D	**(5)***	**12**	**13**		
TH01	**(7)**	**9**	**9.3**		
vWA	**16**	**(17)**	**(18)**	**19**	
D21S11	**29**	**(31.2)**	**32.2**		
D7S820	**(8)**	**10**	**11**	**12***	
D5S818	**12**	**13**			
TPOX	**8**				
DYS391	**10***				
D8S1179	**8**	**10**	**(12)***	**(13)**	
D12S391	**16**	**17.3**	**(19)**	**(22)***	**(23)***
D19S433	**13**	**14**	**(16)**		
FGA	**(20)**	**21**	**(24)***	**27**	
D22S1045	**15**	**(16)**			

Figure 32. Panel A. PowerPlex® Fusion STR typing profile of the pre-sorted fraction of Alexa 647 anti-testosterone mixture. Alleles belonging to the male contributor are highlighted in blue, alleles belonging to the female contributor are highlighted in pink, and alleles that can be contributed to both the male and female profiles are split blue and pink. Alleles that belong to a third contributor are highlighted in white with an asterisk (*). Parentheses (#) denote a minor allele, and [#] denote alleles below analytical threshold.

Panel B

	P5 (Left Post-Sort)	
AMEL	X	
D3S1358	15	19*
D1S1656		
D2S441		
D10S1248		
D13S317	12	
Penta E		
D16S539	10	
D18S51		
D2S1338		
CSF1PO	12	
Penta D		
TH01	7	
vWA	16	19
D21S11		
D7S820		
D5S818		
TPOX		
DYS391		
D8S1179	8	12*
D12S391		
D19S433		
FGA		
D22S1045		

Panel C

	P6 (Right Post-Sort)			
AMEL	X	Y		
D3S1358	15	(16)	(18)	
D1S1656	11	(12)	14	
D2S441	10	11	12*	14
D10S1248	(12)*	13	14	
D13S317	12	[13]		
Penta E	7	11*	[13]	[15]
D16S539	(12)*	13	14	
D18S51	14	15	(20)*	
D2S1338	17	23		
CSF1PO	10	12		
Penta D	10*	12		
TH01	(7)	9	(9.3)	
vWA	16	(17)	(18)	(19)
D21S11	28*	(29)	(32.2)	
D7S820	(8)	10	(11)	
D5S818	11	(12)		
TPOX	8			
DYS391				
D8S1179	(8)	10	(13)	14*
D12S391	(16)	17.3	(18)	
D19S433	(13)	14*	(15)*	
FGA	(19)	20	(21)	(27)
D22S1045	14*	15		

Figure 32. Panel B & Panel C. PowerPlex® Fusion STR typing profile of the P5 post-sort fraction of Alexa 647 anti-testosterone mixture. Panel B. P6 post-sort fraction. Alleles belonging to the male contributor are highlighted in blue, alleles belonging to the female contributor are highlighted in pink, and alleles that can be contributed to both the male and female profiles are split blue and pink. Alleles that belong to a third contributor are highlighted in white with an asterisk (*). Parentheses (#) denote a minor allele, and [#] denote alleles below analytical threshold.

Vita

Kristin Noelle Jones was born on October 27, 1995, in Philadelphia, Pennsylvania. She graduated from Egg Harbor Township High School in Egg Harbor Township, New Jersey in 2010. She received her Bachelor of Science in Forensic Science from Liberty University, Lynchburg, Virginia in 2018. While pursuing her undergraduate degree, Kristin worked as a student researcher in the Liberty University Forensic Science Laboratory on several projects, one of which was later published in the Journal of Forensic Identification in December 2018. Kristin completed her undergraduate degree by interning at the Office of the Chief Medical Examiner in Washington D.C. in their Toxicology Unit, where she worked on novel phencyclidine research that would later be presented at several conferences. While pursuing her graduate degree Kristin became employed at the Virginia Department of Forensic Science in Richmond, where she would also become a Graduate Student Research Intern and complete this dissertation.